CHAPTER 6

DETERMINATION OF COBALT IN A ZINC ELECTROLYTE

6.1) SUPPORTING ELECTROLYTE

The voltammetric determination of cobalt is difficult in the presence of zinc as their reduction potentials are similar in most supporting electrolytes and the resolving power of differential pulse voltammetry is not sufficient to separate these peaks [3]. Electroanalytical methods have been developed for the determination of copper, cadmium, lead, antimony and iron in zinc plant electrolytes [4-7], but these methods are not suitable for the determination of cobalt in the same sample.

There are also problems associated with the determination of cobalt at a mercury electrode, namely, irreversibility of the process and poor sensitivity of stripping methods due to the low solubility of cobalt in mercury [8-10]. Therefore complexing agents have been employed to form a cobalt complex, which is then adsorptively accumulated at the electrode-solution interface prior to the electrode process [8].

The reagent most frequently used for quantitative cobalt determination is dimethylglyoxime (DMG). This forms a complex with the ratio Co:DMG = 1:2 [11]. Due to its surface activity, the $[Co(DMG)_2]$ complex adsorbs onto the electrode surface and thus provides a means of preconcentration. This results in an increased sensitivity [8,12,13]. The mechanism of the electrode process is under dispute for this complex as some believe that the reduction process is accompanied by a catalytic evolution of hydrogen, while the majority maintain that the increase in current is due to the adsorptive accumulation of the complexes on the electrode surface [14].

One of the newest theories on the mechanism for the electrochemical stripping reduction of the cobalt (and nickel) DMG complexes is that by Ma *et al.* [13]. They postulated that it is a 10-electron process in alkaline media. First the complex is adsorbed onto the electrode surface:

$$[Co(II)\text{-}DMG_2]_{(sample)} \rightarrow [Co(II)\text{-}DMG_2]_{(ads)}$$

The central ion is then reduced:

$$[Co(II)\text{-}DMG_2]_{(ads)} + 2e^- \rightarrow Co(0) + 2DMG^-_{(ads)}$$

This is followed by a four-electron reduction of each glyoximate ligand in which hydroxylamine groups are formed:

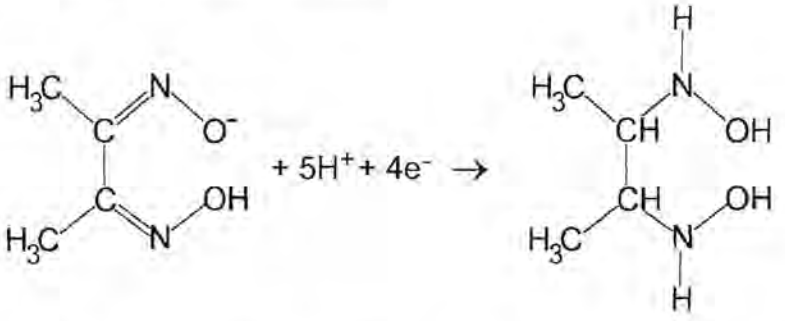

In addition to cobalt(II) the only other metals commonly cited to form stable DMG complexes are nickel(II), copper(II), palladium(II), platinum(II) and bismuth(III) [15]. This should be borne in mind as interferences may not only arise from the overlap of reduction peaks, but could also stem from competitive reactions with the complexing agent and from the competitive adsorption of ions or their complexes on the electrode surface [14]. Thus high concentrations of the other elements which also form complexes with DMG will compete to react with the DMG and possibly for space on the electrode to adsorb too.

Cobalt was determined as a DMG complex in ammonium chloride, but it was susceptible to interference from zinc [3]. The $[Co(DMG)_2]$ complex was also analysed in water with a NH_3-NH_4Cl and $CaCl_2$ supporting electrolyte [16]; or in biological materials [9], pressurised water reactor coolant [12] and iron samples [17] with just a NH_3-NH_4Cl supporting electrolyte [9]; or in water with NH_3 and HEPES (4-(2-hydroxyethyl)-1-piperazineethanesulphonic acid) [18] and so on. A novel way of using the DMG complex to determine cobalt was by making mixed binder carbon paste electrodes (MBCPE) [19]. DMG was mixed with graphite, liquid paraffin and glycerol and made into an electrode. The cobalt in solution then complexes with the DMG on the electrode and once again a sensitive determination for cobalt was produced.

The main disadvantage of using DMG on it own for cobalt determinations is the close proximity of the nickel and especially the zinc reduction peaks to that of cobalt, hence there is strong interference if these elements are present in solution [9,20]. Other complexes, in combination with DMG or on their own, have been studied to overcome problems experienced when using DMG.

The addition of citrate to the DMG and NH_4Cl was used to determine cobalt in an excess of nickel [20]. This approach was extended to overcome the zinc interference, where 2 ppb cobalt could be determined in 150-fold excess of zinc [3,20]. Triethanolamine (TEA) was added to DMG and NH_4Cl to determine cobalt in sea water [21]. It was also used to determine 0.05 $\mu g.l^{-1}$ cobalt in up to 25 000-fold excess of zinc [3]. Tetrabutylammonium fluoride (TBAF) was added to DMG, citrate and NH_4Cl to shift the zinc reduction potential to even more negative values [20]. Diacetyl dioxime (DAD) was also used in this manner [22], but the zinc and cobalt reduction peaks were not sufficiently separated to determine cobalt in a zinc plant electrolyte [22]. The addition of iminodiacetic acid (IDA) was studied as this formed a non-electroactive zinc complex [20]. 1-(benzylsulphonyl)-2-(N-morpholino) ethane (BME) was used to analyse for cobalt in a zinc electrolyte as the Zn^{2+} reduction is retarded without inhibiting the reduction of the cobalt-DMG complex. It was possible to determine 60 $\mu g.l^{-1}$ cobalt in the presence of 40000-fold excess zinc [22]. 2-quinolinethiol has been used to separate the cobalt, nickel and zinc peaks [20]. The use of the cobalt(III)-2-nitroso-1-naphthol complex in an ammoniacal supporting electrolyte made it possible to determine 2 $\mu g.l^{-1}$ cobalt in 1000-fold excess of zinc without interference [3]. Ethylenediamine with KNO_3 was used to determine cobalt in zinc [23]. Both dioxime [14] and nioxime [24], as well as thiocyanate [25], were used in conjunction with nitrite to determine cobalt. The reduction current was catalytically enhanced by the presence of nitrite, thus it was more sensitive. Other complexes studied include oxine [26], nioxime (cyclohexane-1,2-dione dioxime) [14,24,26], α-furil dioxime [14], diphenylglyoxime [24], dithiocarbamate [10], a synthesised azo compound 1-(2-pyridylazo)-2,7-dihydroxynaphthalene (2,7-PADN) [27] and so on.

Although many of the complexes improved the separation between the cobalt and the nickel and zinc peaks, they were insufficient to determine cobalt in a zinc plant

electrolyte as the high zinc concentration interfered. Bobrowski [14] developed a method using α-benzil dioxime as complexing agent which also forms a complex with the ratio of 1:2 for Co: α-benzil dioxime. Cobalt could be determined in solutions containing zinc concentrations 10^7 times higher than that of cobalt. The resolution and sensitiivity were futher enhanced by the addition of the nitrite ion, which, as described before, gives rise to a catalytic effect. Mrzljak *et al.* [10] used this method in determining cobalt in a zinc plant electrolyte and obtained excellent sensitivities, but a very small working range of 0.25 $\mu g.l^{-1}$ to 30 $\mu g.l^{-1}$ cobalt under the specific working conditions were obtained.

Mrzljak *et al.* [10] also looked at a matrix exchange method to determine cobalt in a zinc plant electrolyte using DMG and citrate. This method produced a lower sensitivity, but a wider working range up to 600 $\mu g.l^{-1}$ under the particular conditions. It was decided to look at this electrolyte as it best fitted the requirements for the limits that cobalt could be tolerated in the zinc electrolyte. Below a certain value, the exact concentration is not that critical as it would be below the required lower limit and hence within specifications. The starting point was to look at the same supporting electrolytes as proposed by Mrzljak *et al.* and then to optimise them for the flow system that has been developed.

6.2) ADSORPTIVE STRIPPING VOLTAMMETRY

Adsorptive stripping voltammetry involves the formation of an appropriate metal chelate, followed by its controlled interfacial accumulation onto the working electrode. The adsorbed metal chelate is then reduced by the application of a negative-going potential scan. The reduction can proceed though the metal or the ligand [1]. This technique is very sensitive and only short accumulation times are required.

The amount of adsorbate accumulated at the electrode surface depends on both the size and orientation of the molecule or ions. There are a number of forces leading to adsorption such as: the solubility of the reactant in the solvent (the lower the solubility, the stronger the adsorption), the electrostatic forces between an ionic adsorbate and the charged electrode, the field-dipole interaction between the

electrode double layer and the functional groups of the organic reactant, and the chemisorption of certain groups on metallic electrode surfaces [2].

Adsorption isotherms have been derived to indicate the equilibrium relationships between the concentration of the adsorbate on the surface of the electrode and that in the bulk solution [2]. The most popular of these isotherms in the Langmuir isotherm, given by [1,2]:

$$\Gamma = \Gamma_m \left(\frac{BC}{1+BC} \right)$$

where Γ is the surface concentration of adsorbate, Γ_m is the surface concentration corresponding to monolayer coverage, C is the bulk concentration of adsorbate and B is the adsorption coefficient. From this it can be deduced that when $BC<<1$, $\Gamma = \Gamma_m BC$. In other words, when the adsorbate concentration is very low, its surface concentration is directly proportional to its bulk concentration [2]. The Langmuir isotherm does not always apply. For example, it does not take the interactions between the adsorbate on the electrode surface into account. Therefore there are more complex isotherms.

For AdSV, the peak current is directly proportional to the surface concentration of the adsorbate at low concentrations. At high concentrations, a deviation from linearity is evident which is due to the electrode surface approaching full surface coverage and becoming saturated with adsorbate. To extend the linear range, the sample can be diluted, a shorter preconcentration time can be used or the rate of forced convection can be reduced. It is suggested that when using a method of standard addition, three additions be made to ensure that the response lies within the linear range [2].

6.3) BACKGROUND

The work by Mrzljak *et al.* [10] was used as a basis for this part of the project. The flow system designed was tested by using a proven flow method. The flow system could then be used in other trace determinations in various complex matrices.

Their work takes many factors into account. The cobalt sensitivity was enhanced by forming the DMG complex and hence AdSV was employed. The interference from

the extremely high zinc concentrations present were reduced in two ways, namely, by complexing the zinc with sodium citrate which moved the zinc reduction peak to more negative potentials and by utilising a matrix exchange method where stripping occurred in a comparatively uncontaminated solution. [10]

Mrzljak *et al.* [10] used a bottom-drain cell displayed in figure 6.1. The zinc electrolyte was first diluted six times with a supporting electrolyte. The sample was then injected directly over the HMDE from the flow adapter and during that time the analyte was collected at the working electrode that was held at a fixed potential. Due to the greater density of the sample versus the stripping electrolyte contained in the cell, the sample sank to the bottom of the cell and stripping occurred in a relatively uncontaminated solution, thus reducing zinc interference. The contaminated stripping electrolyte was then drained and replaced by fresh electrolyte [10]. This cell design restricted its use to samples more dense than the stripping electrolyte, whereas the cell design for this project was aimed at producing a cell that would be more versatile.

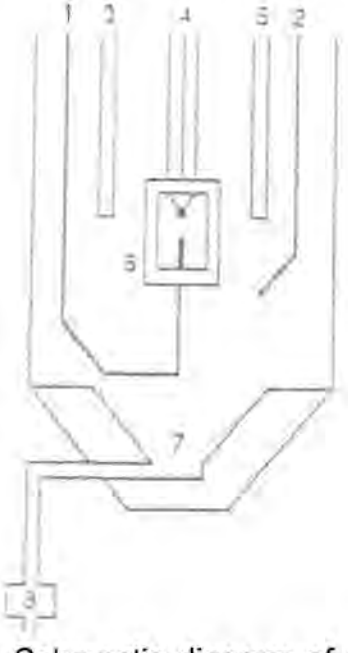

Figure 6.1: Schematic diagram of the bottom-drain cell used by Mrzljak *et al* [10]. (1) Sample inlet line; (2) nitrogen purge line; (3) reference electrode; (4) Metrohm HMDE; (5) auxiliary electrode; (6) PAR 310 flow adapter; (7) sample-electrolyte drain to waste; (8) control valve

The composition of the supporting and the stripping electrolytes are given in table 6.1. It was decided to begin this work with the same compositions and then to optimise the components.

Table 6.1: The composition of the supporting and the stripping electrolytes as used by Mrzljak *et al.* [10]

	Supporting electrolyte	Stripping electrolyte
Trisodium citrate	0.5 mol.l^{-1}	0.1 mol.l^{-1}
Ammonia	0.4 % (v/v)	0.04 % (v/v)
Ammonium chloride	-	0.1 mol.l^{-1}
DMG	5 x 10^{-4} mol.l^{-1}	3 x 10^{-3} mol.l^{-1}
pH	6.4	8.4

In the current project, a synthetic zinc electrolyte was used so that the contaminants could be controlled. This was made up according to the typical feed electrolyte found at Zincor. It consisted of 140 g.l^{-1} zinc, 10 g.l^{-1} manganese, 10 g.l^{-1} magnesium and 0.7 g.l^{-1} calcium. This was in a sulphate medium so the sulphate salts were used and the pH was adjusted to 5.

6.4) EXPERIMENTAL AND RESULTS

6.4.1) Supporting and Stripping Electrolyte Compositions

The composition of the supporting and stripping electrolytes is important as it reduces interference, enhances sensitivity, reduces resistance and so on. The compositions of these electrolytes were optimised for the designed flow system.

6.4.1.1) Sodium Citrate Concentration

Due to the large concentration of zinc present in the sample electrolyte, it was necessary to reduce the extent of interference. Sodium citrate was added to complex the zinc, thus reducing interference by shifting the zinc reduction peak potentials more negative. However, the presence of sodium citrate reduces the cobalt response, hence its concentration was reduced in the stripping electrolyte [10].

The concentration of the sample, and hence the zinc, was also reduced by diluting 4 ml and making it up to 25 ml with the supporting electrolyte.

The concentration of sodium citrate in the stripping electrolyte was investigated by looking at the effect it had on the zinc reduction peak. Matrix exchange DPSV was used with the following parameters:

Initial potential = -600 mV
Final potential = -1100 mV
Deposition time = 5 s
Scan rate = 10 $mV.s^{-1}$
Pulse amplitude = 50 mV
Sample width = 20 ms
Pulse width = 50 ms
Pulse period = 200 ms
Quiet time = 20 s
Drop size = medium
Flow rate = 1.5 $ml.min^{-1}$

The flow system describe in chapter 5 was used with deoxygenation taking place. The solutions were positioned at the selection valve as follows: position 1 was water for rinsing, position 2 was nitrogen, position 3 was the sample already diluted with the supporting electrolyte and position 4 was the stripping electrolyte. The FlowTEK procedure used is depicted in figure 6.2. The peak currents quoted were an average of 3 to 5 measurements and iR compensation was always used.

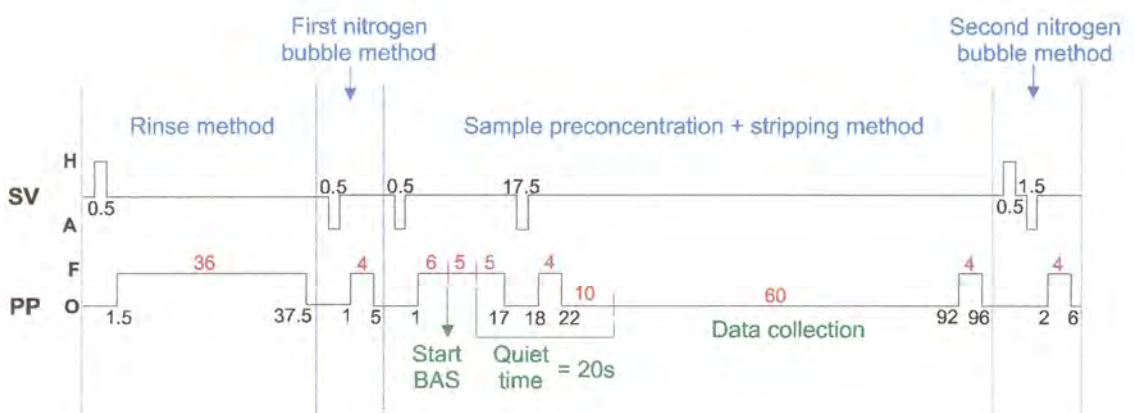

Figure 6.2: Schematic diagram of the FlowTEK procedure with a 5 s adsorption time

The supporting and stripping electrolytes were made up as specified in table 6.1, except the sodium citrate concentration in the stripping electrolyte was varied. The voltammograms in figure 6.3 indicate that varying the concentration of sodium citrate in the stripping electrolyte did not affect the zinc peak much, therefore it could be omitted from this solution. This is beneficial to the sensitivity of the cobalt reduction peak as mentioned above. This result was not surprising because when using the bottom-drain cell, there could still have been zinc in the stripping electrolyte as the only separation mechanism between the sample and stripping electrolyte was the difference in specific gravities. In the flow cell used in this study, the sample was washed out of the cell, so there could only be trace amounts zinc left behind. The slight positive potential shift at the lower citrate concentrations would not be sufficient to interfere with the cobalt reduction peak.

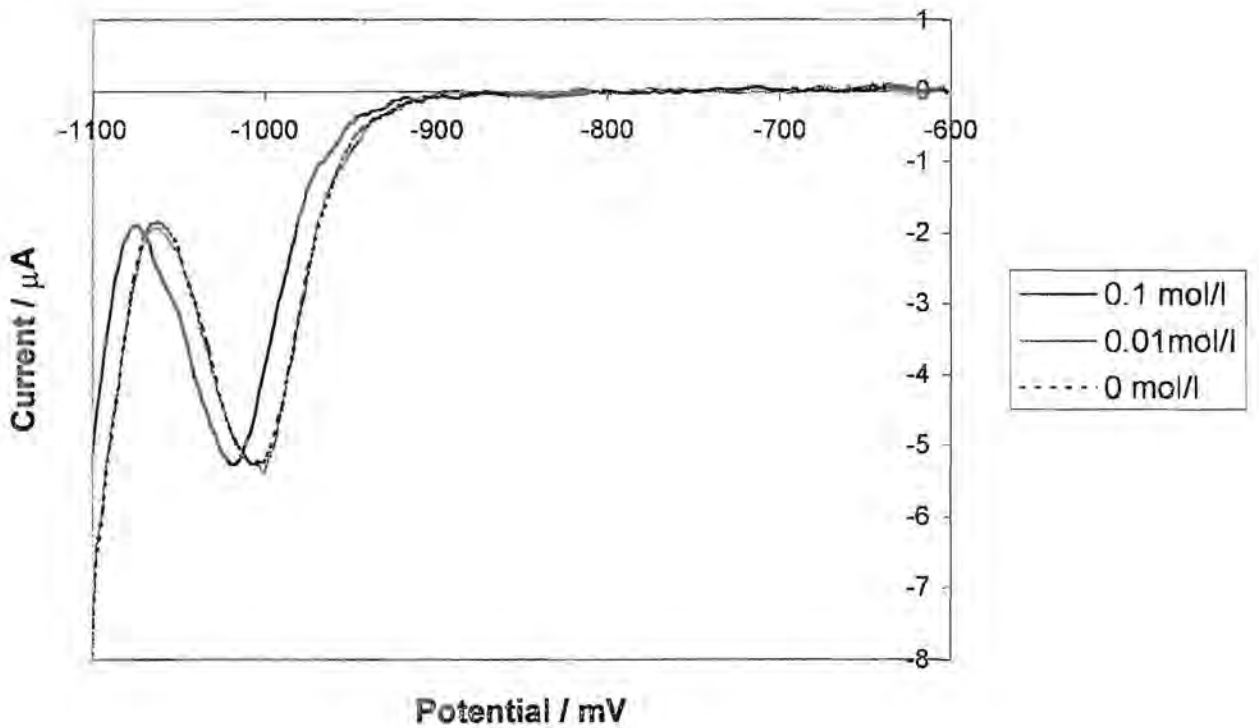

Figure 6.3: Voltammograms showing the effect of varying the sodium citrate concentration in the stripping electrolyte

Varying the concentration of sodium citrate in the supporting electrolyte was then perused under the same conditions as above. The voltammograms in figure 6.4 show that a high concentration of sodium citrate was essential to reduce the interference of the large concentration of zinc present by shifting the zinc reduction

peak to more negative potentials. A concentration of 0.5 mol.l^{-1} was thus used in future work.

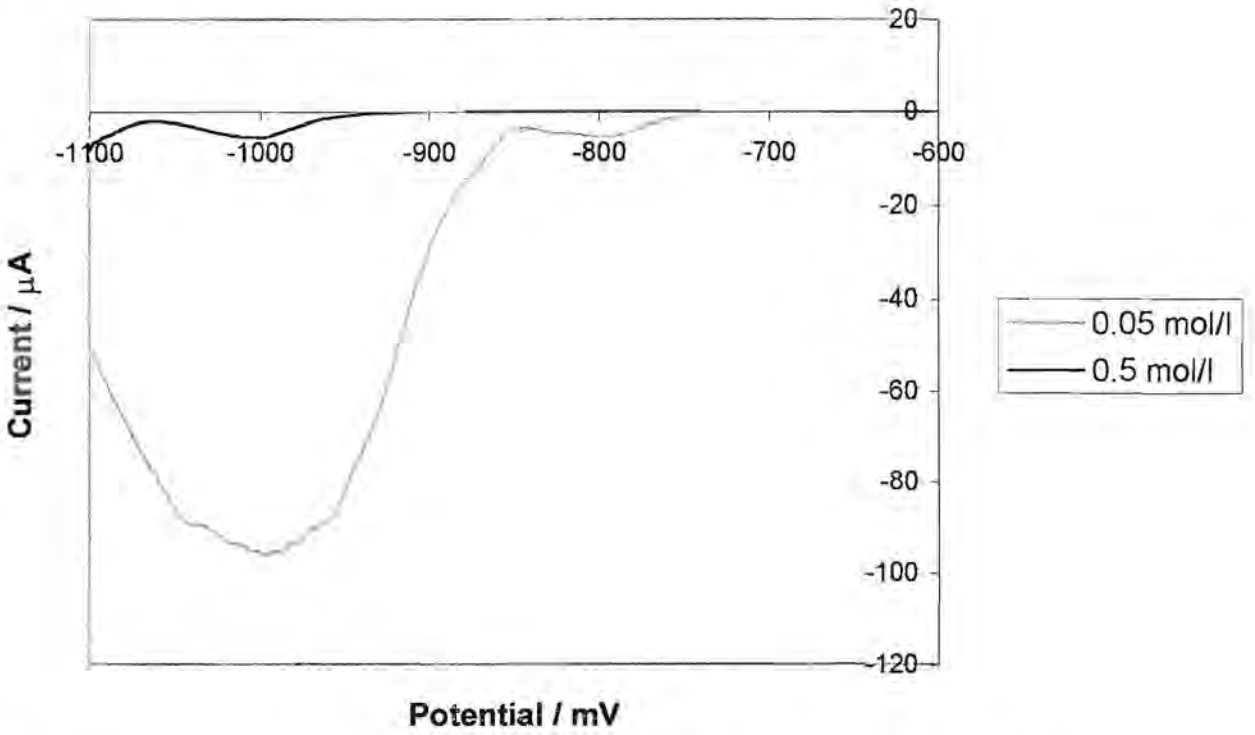

Figure 6.4: Voltammograms showing the effect of varying the sodium citrate concentration in the supporting electrolyte

6.4.1.2) pH

The optimum pH for determining cobalt is between 8 and 9, but precipitates in the zinc electrolyte are formed under those basic conditions. The pH of the complexing electrolyte was kept at a pH of 6.4 by Mrzljak *et al.* [10], where precipitates were not formed but the $[Co(DMG)_2]$ complex was still formed. Stripping could then occur at a more basic pH of 8.4 to increase the sensitivity of the determination.

The pH of the supporting electrolyte was considered in order to improve the sensitivity. A zinc electrolyte containing 1 mg.l^{-1} cobalt was used and the conditions were the same as those used previously, but with a 20 s accumulation time. An increase in pH from 6.4 to 6.7 led to an increase in the peak height of the cobalt peak as seen in figures 6.5 and 6.6. The increase in peak height became more significant at the higher pH values. It was decided not to look at even higher pH values as the limiting factor was the formation of basic precipitates. There was no visible

precipitation at pH 6.7 in the synthetic zinc electrolyte, but a real zinc electrolyte could behave differently. Any slight precipitation could also lead to blocking of tubes in the flow system which had to be avoided. When dealing with a real sample, it would be advantageous to use the highest pH tolerated before precipitation occurs. For the synthetic sample the pH of the supporting electrolyte was thus kept at 6.4 in order to deal with the worst scenario for the real sample.

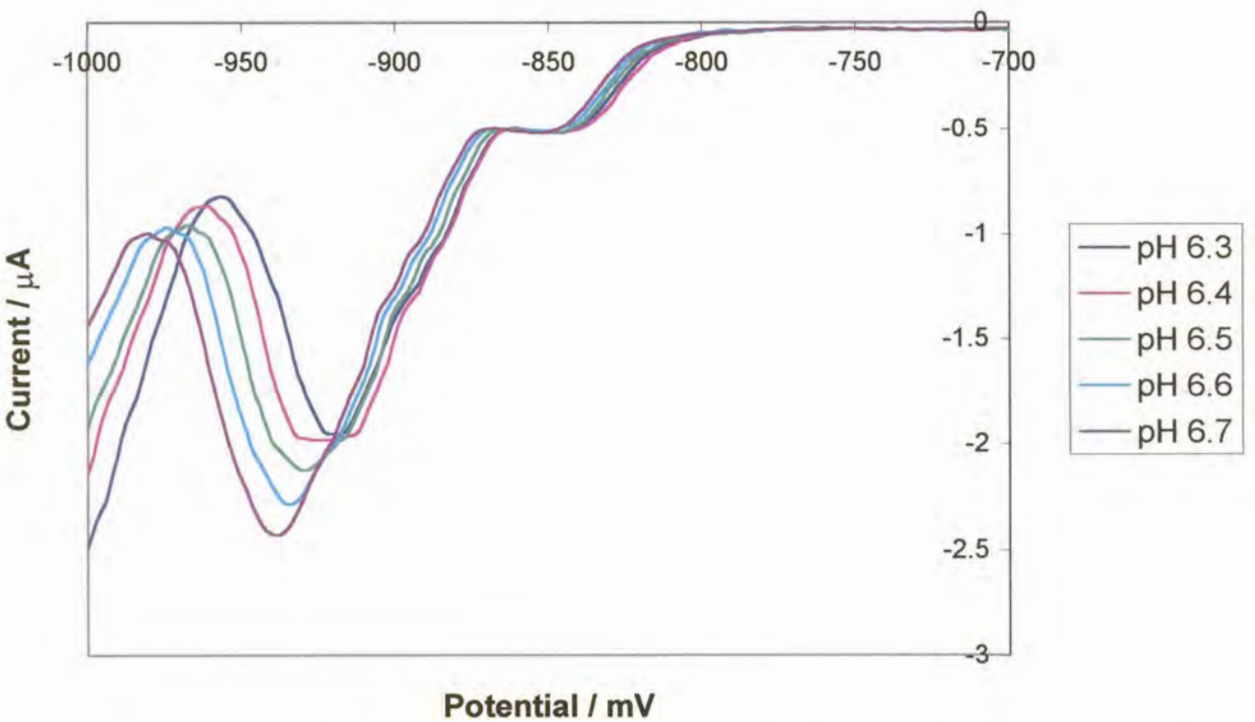

Figure 6.5: Voltammograms showing the effect of varying the pH of the supporting electrolyte

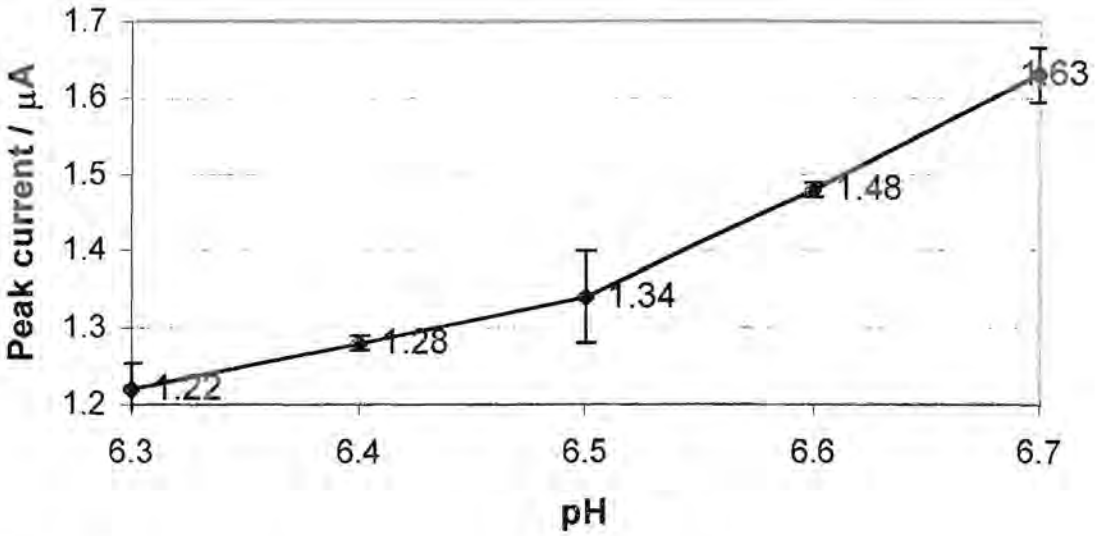

Figure 6.6: Graph of peak current versus pH of the supporting electrolyte

6.4.1.3) Cobalt Concentration

It was decided at this point to look if the change in peak height with cobalt concentration in a zinc electrolyte would yield a linear curve. The DPSV parameters were the same as before, but a deposition time of 20 s was used. The voltammograms are shown in figure 6.7. As depicted in figure 6.8, a linear curve was produced for the cobalt concentration of 0.2 to 1 $mg.l^{-1}$, yielding a correlation coefficient of 0.9979. A 0.1 $mg.l^{-1}$ cobalt concentration did not produce a peak for a 20 s deposition time, thus a longer deposition time would be required for greater sensitivity.

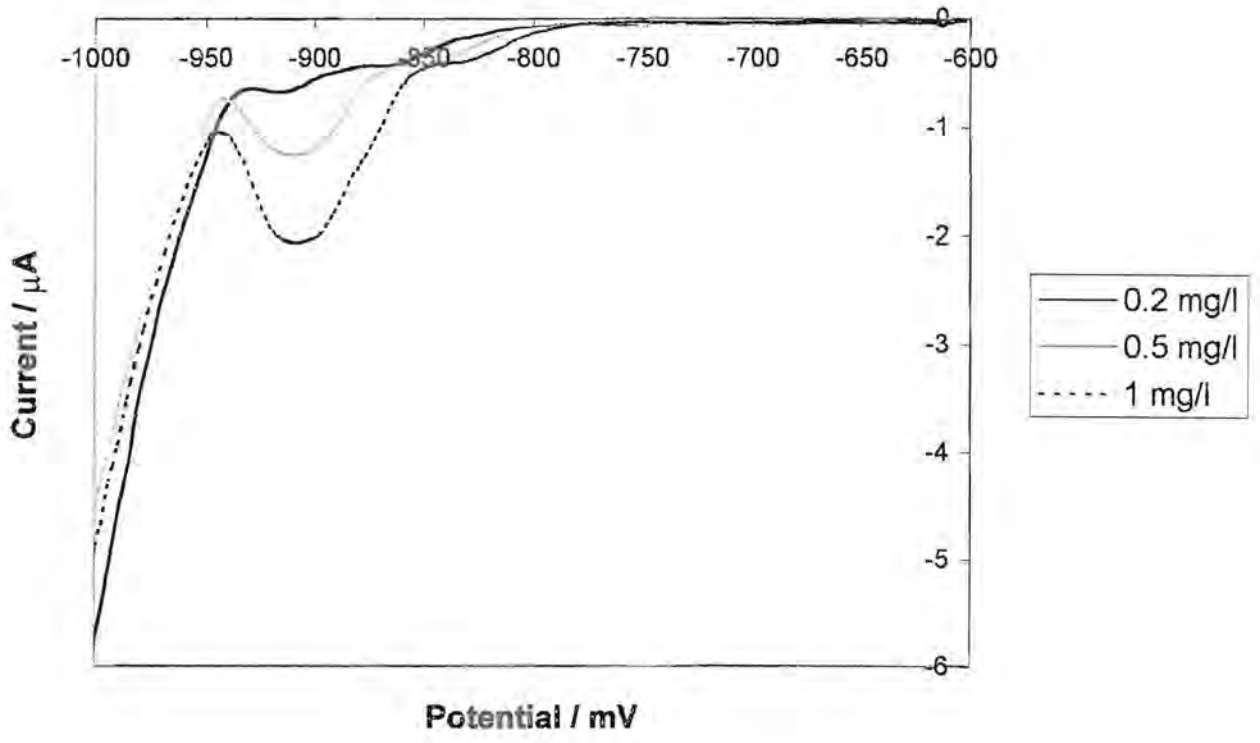

Figure 6.7: Voltammograms showing the effect of varying the cobalt concentration in the zinc electrolyte

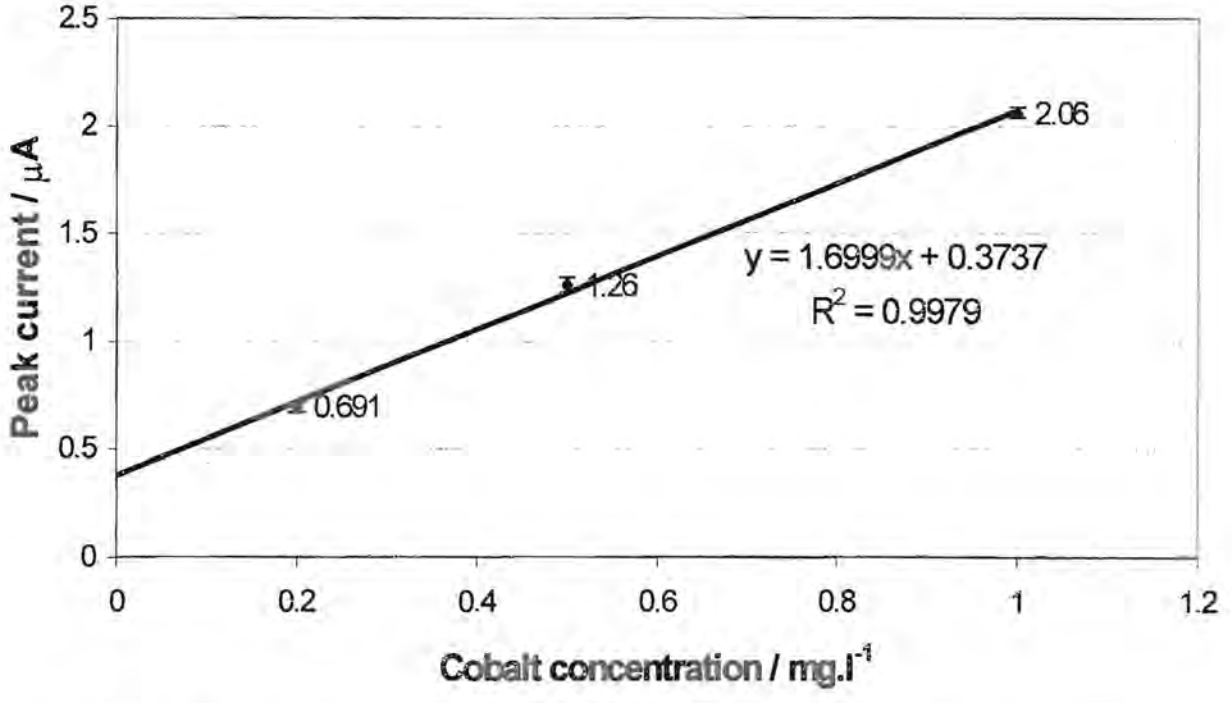

Figure 6.8: Graph of peak current versus cobalt concentration in a zinc electrolyte

6.4.1.4) DMG Concentration

The concentrations of DMG in the supporting and stripping electrolytes were investigated. The conditions were the same as before, but a 20 s deposition time and a 0.5 $mg.l^{-1}$ cobalt concentration in the zinc electrolyte were used. First the DMG concentration in the adsorbing electrolyte was varied as shown in figure 6.9. In the original work a $5x10^{-4}$ $mol.l^{-1}$ DMG concentration was used. From the voltammograms in figure 6.9 it can be seen that at lower DMG concentrations the cobalt peak is not seen, and that the peak height is greater for a $1x10^{-3}$ $mol.l^{-1}$ DMG concentration. This may have been related to the ratio of cobalt to DMG concentration. The initial drop in current, before a steady current was reached, could have been obscuring the cobalt peak at lower DMG concentrations, however it seemed unlikely. This change in current was due to some redox reaction of a component of the background electrolyte. Thus an increase in DMG concentration enhances the sensitivity for cobalt determination. A DMG concentration of $1x10^{-3}$ $mol.l^{-1}$ was used in further work.

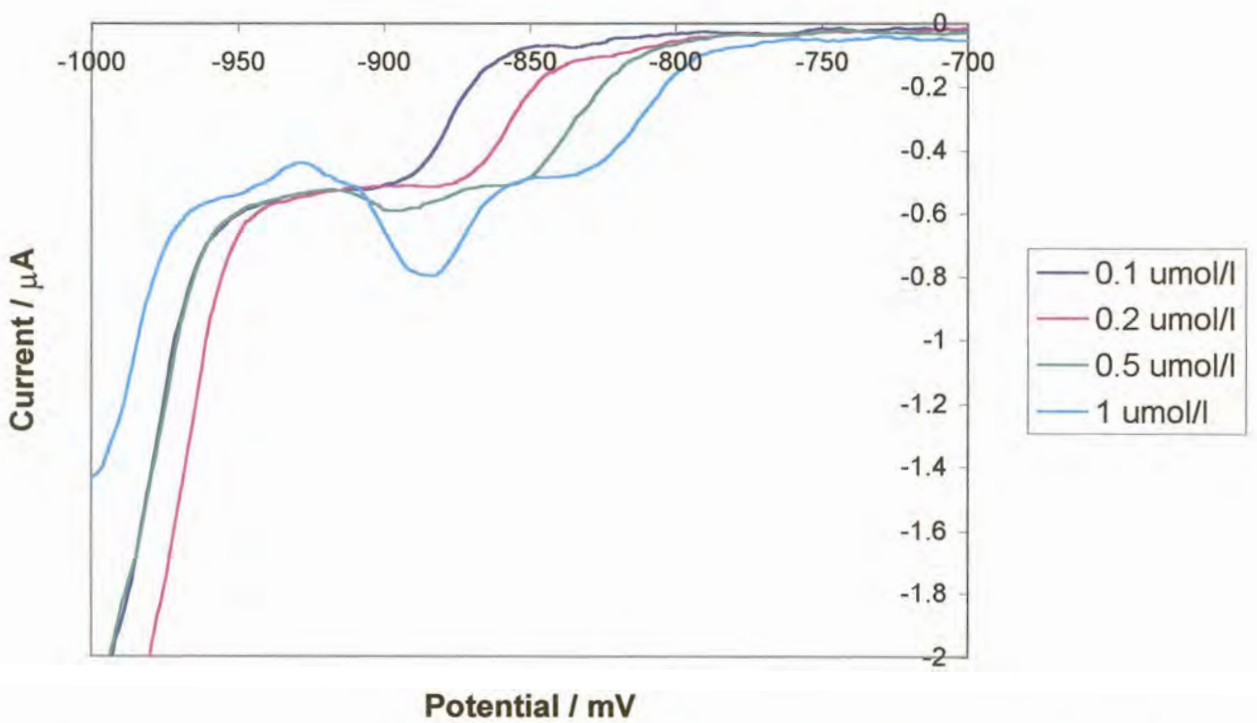

Figure 6.9: Voltammograms showing the effect of varying the DMG concentration in the supporting electrolyte

The influence of the DMG concentration in the stripping electrolyte was also explored. The conditions were the same as that for the above experiment, but the DMG concentration in the stripping electrolyte was varied from $5x10^{-4}$ mol.l^{-1} to $5x10^{-3}$ mol.l^{-1}. The results are depicted in figures 6.10. It was found that the lower the DMG concentration in the stripping electrolyte, the lower the sensitivity for the cobalt reduction peak. The peak heights did not differ much when the electrolyte contained $3x10^{-3}$ mol.l^{-1} DMG versus $5x10^{-3}$ mol.l^{-1} DMG. This was due to the incomplete dissolution of the DMG at the higher concentration. Thus a concentration of $3x10^{-3}$ mol.l^{-1} DMG was used in further work.

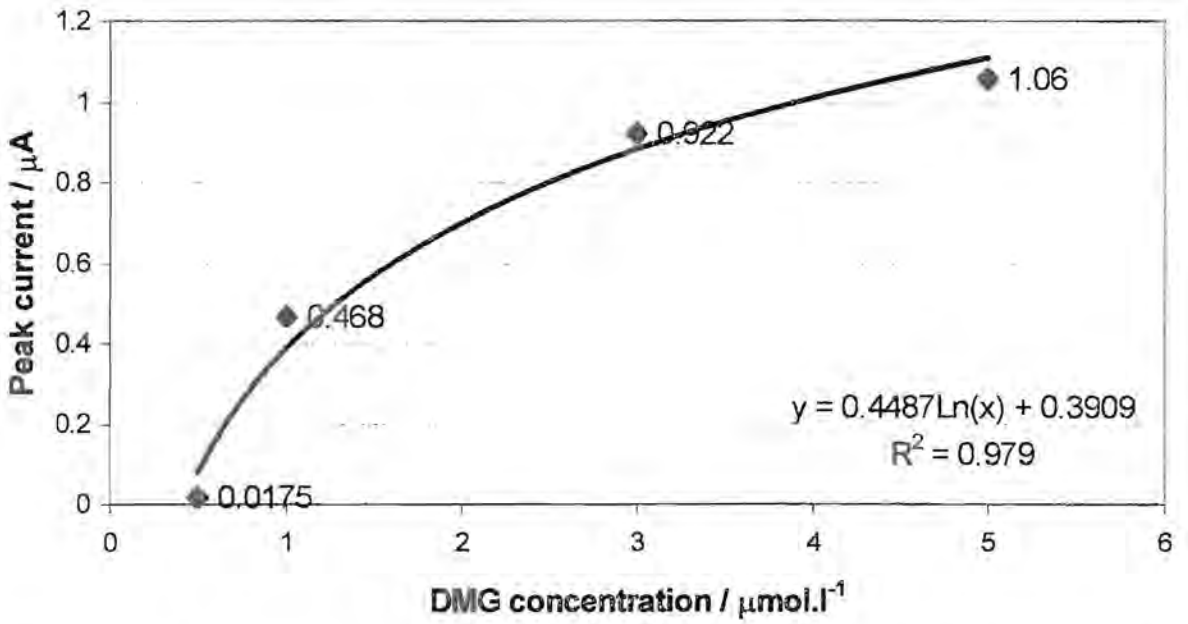

Figure 6.10: Graph of peak current versus DMG concentration in the stripping electrolyte

6.4.1.5) Dilution Factor of the Zinc Electrolyte

The zinc electrolyte was diluted 6.25 times by the supporting electrolyte. In other words, if a zinc electrolyte sample contained 0.25 mg.l^{-1} of cobalt, after the dilution 40 µg.l^{-1} of cobalt needs to be detected. It was therefore decided to see if it was feasible to make a smaller dilution. The function of the dilution was not only to introduce the supporting electrolyte, but also to reduce the zinc concentration and so reduce interference; thus it could not be too small. The usual dilution was 4 ml sample made up to 25 ml with supporting electrolyte. This was compared to taking 6

ml, 8 ml and 10 ml respectively and making it up to 25 ml in each case. In the case of 8 ml and the 10 ml sample aliquot, precipitation occurred at a pH of 6.4. Using a lower pH would not be beneficial to improving the sensitivity as conditions need to be favourable for cobalt-DMG complex formation. The conditions were the same as before and the cobalt concentration in the zinc electrolyte was 0.25 $mg.l^{-1}$. Thus the results for a 6.25 and a 4.17 times dilution were compared and are shown in figure 6.11. It should be noted that not only do the cobalt and zinc concentrations increase, but the concentrations of the various constituents in the supporting electrolyte also decrease. The voltammograms displayed an increase in the cobalt reduction peak height which indicates that a smaller dilution could be made if greater sensitivity was needed. However, once again it would be necessary to ensure that no precipitation occurred for a smaller dilution when analysing a real sample. The concentration of the various components in the supporting electrolyte could also be adjusted so that the different dilution does not affect the resultant concentrations.

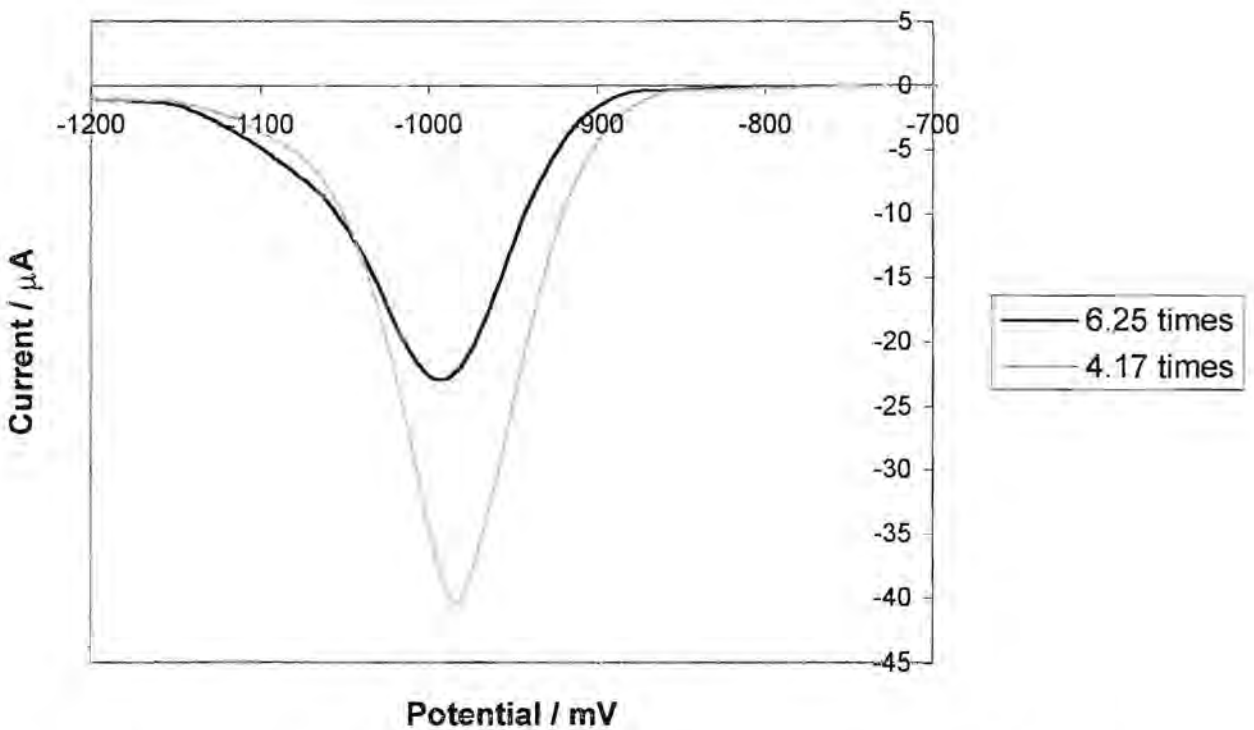

Figure 6.11: Voltammograms showing the effect of varying the sample dilution factor

6.4.2) Experimental Conditions

Not only is the composition of the supporting and stripping electrolytes important, but so are the experimental conditions such as the deposition time, the deposition potential, the potential wave form and so on.

6.4.2.1) Adsorption Time

The FlowTEK methods used for various adsorption times are depicted in figures 6.12 to 6.15. These show how the rinse times were adjusted in order for the solutions to fit in the deoxygenation tubing. A 1 $mg.l^{-1}$ cobalt concentration in the zinc electrolyte was studied. The conditions were the same as that used in the above work.

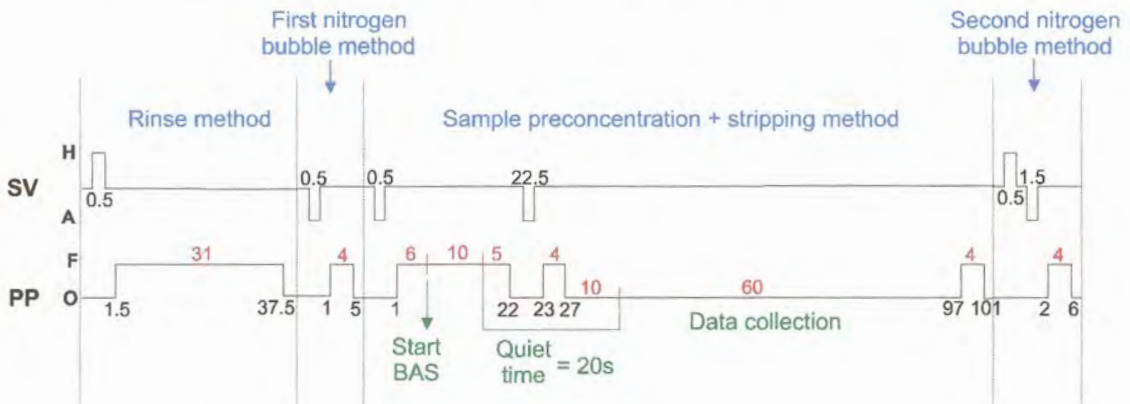

Figure 6.12: Schematic diagram of the FlowTEK method used for a 10 s adsorption time

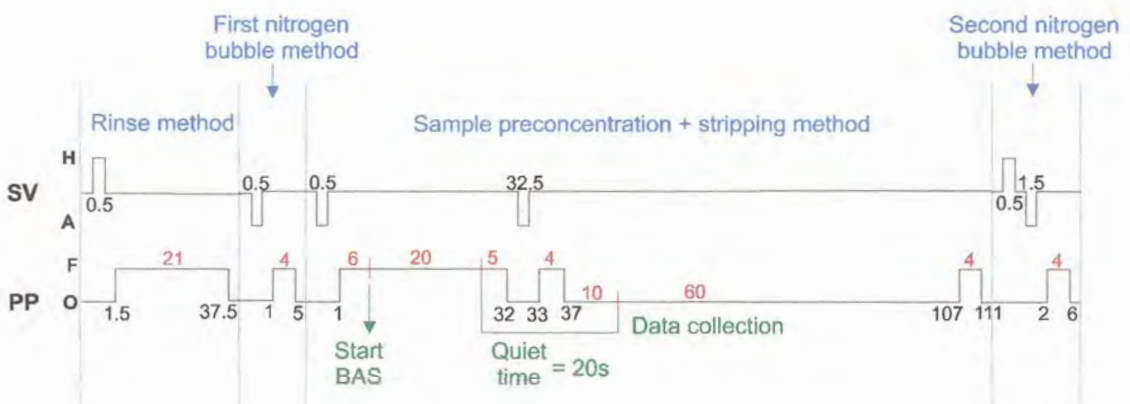

Figure 6.13: Schematic diagram of the FlowTEK method used for a 20 s adsorption time

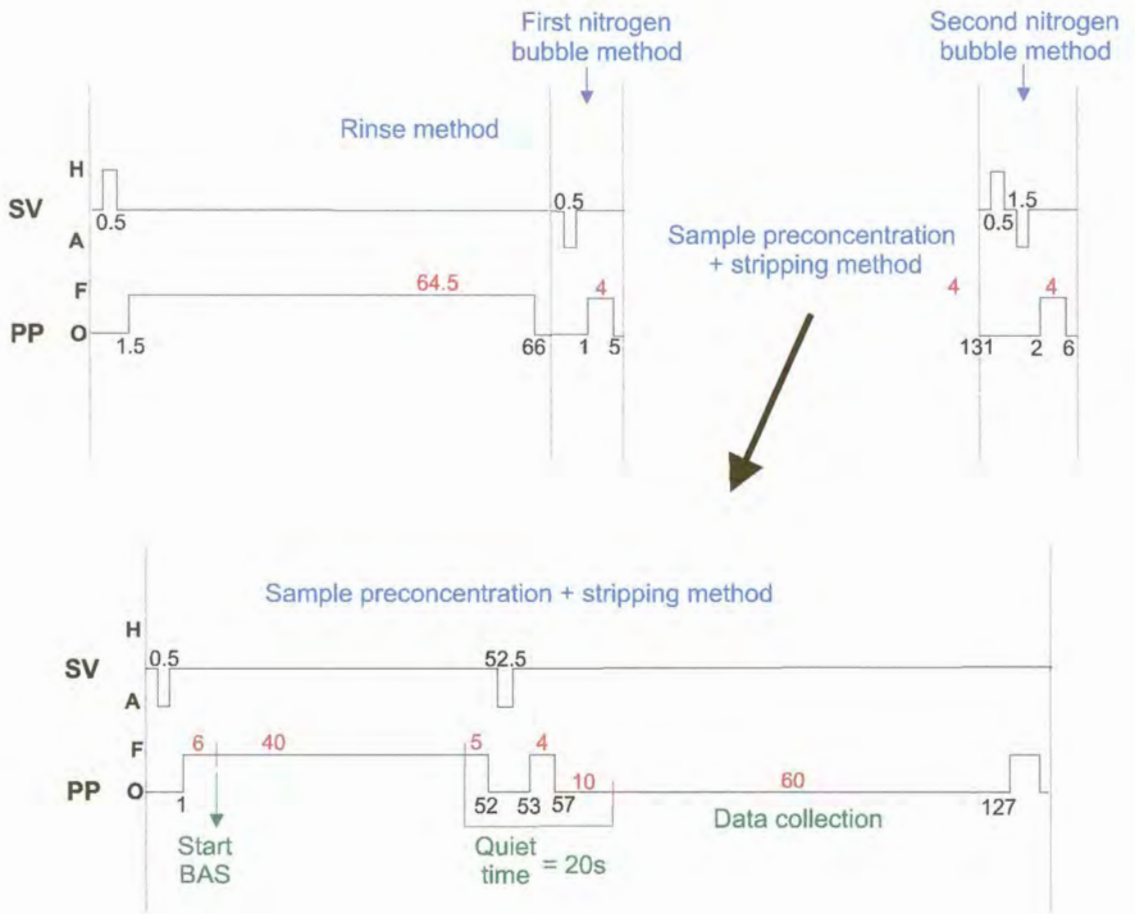

Figure 6.14: Schematic diagram of the FlowTEK method used for a 40 s adsorption time

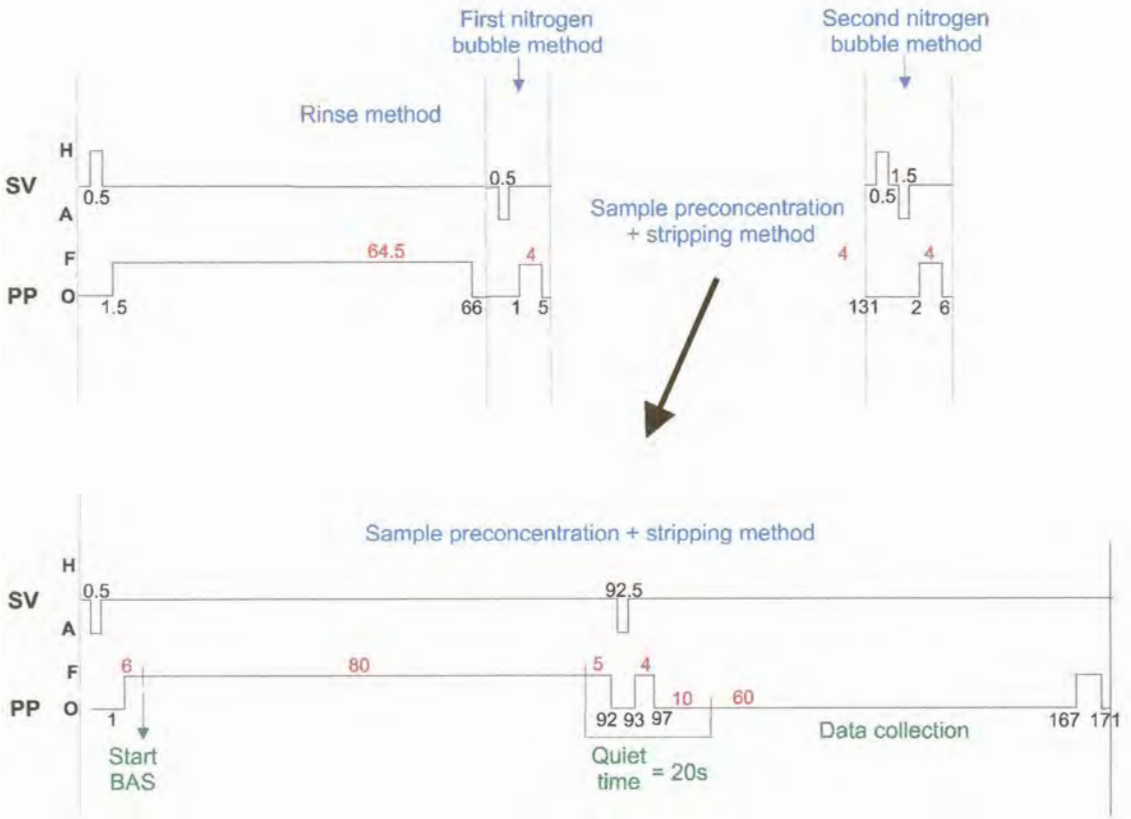

Figure 6.15: Schematic diagram of the FlowTEK method used for a 80 s adsorption time

The results obtained were somewhat erratic as shown in figures 6.16 and 6.17. There were various factors that could contribute to the erratic behaviour, such as the varying rinse times, starting a run when the position of the solution in the flow cell was at different points, the saturation coverage of the electrode surface by the complex and so on. However, the most probable explanation would be the relative positioning of the solution in the flow cell. A way to overcome this problem would be to ensure that when analysing a sample, a method of standard addition is used and that all the conditions remain consistent throughout the determination.

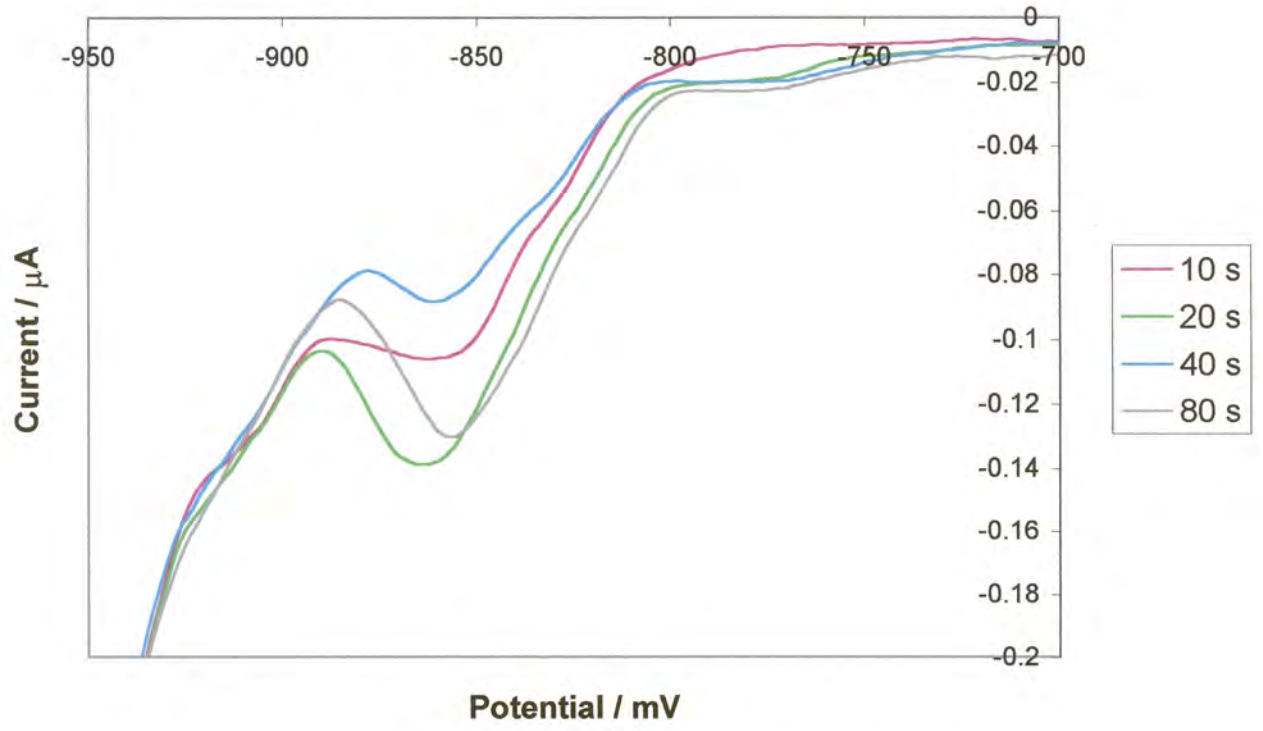

Figure 6.16: Voltammograms showing the effect of varying the adsorption time

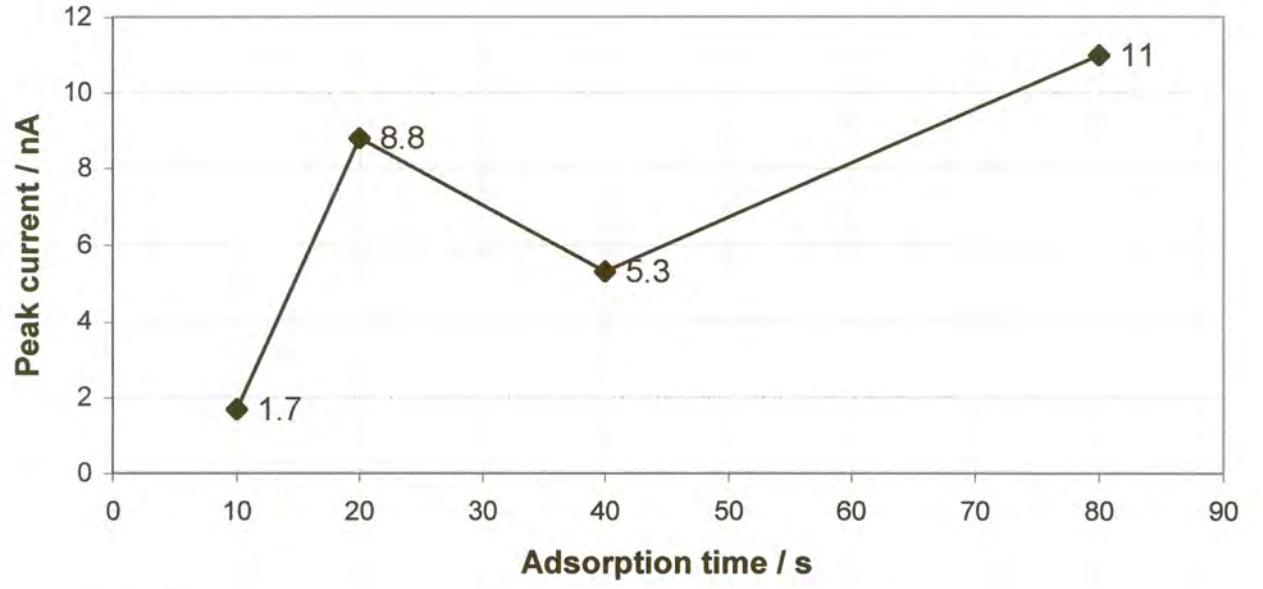

Figure 6.17: Graph of peak current versus adsorption time

6.5) DISCUSSION

In summary, the composition of the supporting and stripping electrolytes is given in table 6.2. Increasing the pH of the supporting electrolyte and diluting the sample to a lesser extent would be preferable if no precipitation occurs.

Table 6.2: The composition of the supporting and the stripping electrolytes

	Supporting electrolyte	Stripping electrolyte
Trisodium citrate	0.5 mol.l^{-1}	0 mol.l^{-1}
Ammonia	0.4 % (v/v)	0.04 % (v/v)
Ammonium chloride	-	0.1 mol.l^{-1}
DMG	1 x 10^{-3} mol.l^{-1}	3 x 10^{-3} mol.l^{-1}
pH	6.4	8.4

The method provided sufficient separation of the zinc and cobalt peaks, even when the amount of zinc present was more than 10^6 times that of the amount of cobalt present. The other main interference, which was not considered in this work, is that from nickel. Nickel and cobalt behave similarly under the conditions of the experimental work, as nickel also forms a $[Ni(DMG)_2]$ complex which is adsorbed onto the electrode and would interfere if present at high concentrations. At least the sensitivity for the $[Co(DMG)_2]$ complex was greater than for the $[Ni(DMG)_2]$ complex under the same conditions [28]. The use of higher ammonium buffer concentrations reduced the amount of interference by increasing the peak separation between the nickel and cobalt reduction peaks, as well as depressing the nickel signal [9,10]. It was shown that varying the ratio of cobalt to nickel concentration led to the interdependent influencing of the respective peak heights due to competition between nickel and cobalt for DMG [28]. The change in nickel concentration only had a slight effect on the cobalt peak height, but the change in cobalt concentration had a more severe effect on the nickel peak height. This effect was reduced by employing a matrix exchange method. It was, however, shown that the nickel levels in the zinc plant electrolyte were too low to be problematic [10].

One of the main problems experienced was that the cobalt reduction peak height did not increase with an increase in the adsorption time. Rather the results obtained

were erratic and showed no trend. This was ascribed most probably to the relative positioning of the solution in the flow cell varying with the different FlowTEK methods used. The longer adsorbing times could also have led to a more pronounced effect from turbulent flow in the flow cell. Employing a method of standard addition when analysing a sample and ensuring that all the conditions remain constant throughout the determination could obviate the problem. However, this is not an ideal situation.

The cobalt reduction peaks produced were very broad and span about 100 mV which is not ideal for analytical purposes. When considering the complicated matrix in which this determination is performed, however, the fact that there was no interference from the large excess of zinc present is significant. The cobalt peak potential occurred between 900 mV and 950 mV. The peak would have been totally overlapped by that for zinc if sodium citrate was not introduced as a complexing agent for the zinc. A fair sensitivity was obtained for cobalt and 0.2 $mg.l^{-1}$ could be determined with an accumulation time of only 20 s. As mentioned previously, due to the dilution of the sample an actual concentration of 32 $\mu g.l^{-1}$ was detected. Mrzljak *et al.* [10] estimated that 0.3 $mg.l^{-1}$ cobalt could be tolerated in the presence of other impurities, thus the detection limit for these conditions was sufficient.

A persistent concern throughout this work was that the resistance was measured between 200 Ω to 300 Ω, when calculating the iR compensation. This resistance seemed to be high for the conducting electrolyte solution in which it was measured. The high resistance was found in both the flow cell and the normal cup cell, when using different capillaries, when using different mercury, when using different electrodes and so on. It seemed that there was probably a dirty contact somewhere in the SMDE causing the problem.

Mechanical failure of the SMDE prevented real samples from being considered, as well as other matrices from being studied using this flow system. This work did, however, show that it was possible to determine impurities in complex matrices by employing electrochemical techniques.

6.6) REFERENCES

1) P.T. Kissinger and W.R. Heineman, Laboratory Techniques in Electroanalytical Chemistry, 2nd edition, Marcel Dekker Inc., New York, 1996
2) A.J. Bard, Electroanalytical Chemistry, Volume 16, Marcel Dekker Inc., New York, 1989
3) M. Geissler and R. Da Maia, Fresenius Z. Anal. Chem., 330 (1988) 624
4) A.M. Bond, R.W. Knight and O.M.G. Newman, Anal. Chem., 60 (1988) 2445
5) A.M. Bond, H.A. Hudson, D.L. Luscombe, K.L. Timms and F.L. Walter, Anal. Chim. Acta, 200 (1987) 213
6) M. Geissler and R. Kunze, Fresenius Z. Anal. Chem., 318 (1984) 15
7) A.M. Bond, B.V. Pfund and O.M.G. Newman, Anal. Chim. Acta, 277 (1993) 145
8) B. Pihlar, P. Valenta and H.W. Nurnberg, Fresenius Z. Anal. Chem., 307 (1981) 337
9) S.B. Adeloju, A.M. Bond and M.H. Briggs, Anal. Chim. Acta, 164 (1984) 181
10) R.I. Mrzljak, A.M. Bond, T.J. Cardwell, R.W. Cattrall, R.W. Knight, O.M.G. Newman, B.R. Champion, J. Hey and A. Bobrowski, Anal. Chim. Acta, 281 (1993) 281
11) I.V. Pyatnitskii, Analytical Chemistry of Cobalt, Oldbourne Press, 1966
12) K. Torrance and C. Gatford, Talanta, 32 (1985) 273
13) F. Ma, D. Jagner and L. Renman, Anal. Chem., 69 (1997) 1782
14) A. Bobrowski, Anal. Chem., 61 (1989) 2178
15) R.P. Baldwin, J.K. Christensen and L. Kryger, Anal. Chem., 58 (1986) 1790
16) M.I. Abdullah and L.G. Royle, Anal. Chim. Acta, 58 (1972) 283
17) A. Economou and P.R. Fielden, Talanta, 46 (1998) 1137
18) J.A. Herrera-Melian, J.M. Dona-Rodriguez, J. Hernandez-Brito and J. Perez-Pena, J. Chem. Ed., 74 (1997) 1444
19) Z.-Q. Zhang, H. Liu, H. Zhang and Y.-F. Li, Anal. Chim. Acta, 333 (1996) 119
20) M.G. Paneli and A. Voulgaropoulos, Fresenius J. Anal. Chem., 341 (1991) 716
21) H. Zhang, R. Wollast, J.-C. Vire and G.J. Patriarche, Analyst, 114 (1989) 1597
22) T. Schmidt, M. Geissler, G. Werner and H. Emmons, Fresenius Z. Anal. Chem., 330 (1988) 712
23) E.S. Pilkington, C. Weeks and A.M. Bond, Anal. Chem., 48 (1976) 1665
24) M. Vega and C.M.G. van den Berg, Anal. Chem., 69 (1997) 874
25) Z. Goa, K.S. Siow and L. Yeo, Anal. Chim. Acta, 320 (1996) 229

26) Colombo and C.M.G. van den Berg, Anal. Chim. Acta, 337 (1997) 29

27) Z.-Q. Zhang, S.-Z. Chen, H.-M. Lin and H. Zhang, Anal. Chim. Acta, 272 (1993) 227

28) R.I. Mrzljak, A.M. Bond, T.J. Cardwell, R.W. Cattrall, R.W. Knight, O.M.G. Newman and B.R. Champion, Analyst, 119 (1994) 1057

CHAPTER 7

DETERMINATION OF ARSENIC IN HIGH PURITY GOLD

7.1) DISSOLUTION OF GOLD IN CYANIDE

The following excerpt [1] shows how long ago it was found that gold could be dissolved in a cyanide solution: "The first definite report of solubility of gold in an aqueous solution of an alkali-metal cyanide is given in a memoir by K.W. Scheel, published in 1783, and in 1846 the importance of oxygen in the dissolution was recognised." Many have studied the mechanisms by which the dissolution occurs and tried to optimise conditions for dissolution [2-9].

Gold will readily dissolve in dilute solutions of alkali-metal cyanide where concentrations of 0.05% to 0.2% are used to leach gold from its ore [1,10]. The $[Au(CN)_2]^-$ complex formed is extremely stable, with a stability constant of $2x10^{38}$ [11].

The accepted reaction mechanism is given as [1,2,11]:

$$4Au + 8CN^- + O_2 + 2H_2O = 4[Au(CN)_2]^- + 4OH^-$$

However, the reduction of oxygen to the hydroxide ion occurs via a hydrogen peroxide intermediate as shown [11]:

$$O_2 + 2H_2O + 2e^- = H_2O_2 + 2OH^-$$

$$H_2O_2 + 2e^- = 2OH^-$$

As H_2O_2 is a strong oxidant, it also promotes the formation of $[Au(CN)_2]^-$. Thus the intermediate route could be as follows:

$$2Au + 4CN^- + O_2 + 2H_2O = 2[Au(CN)_2]^- + 2OH^- + H_2O_2$$

$$2Au + 4CN^- + H_2O_2 = 2[Au(CN)_2]^- + 2OH^-$$

The mechanism is evidently electrochemical [1,2].

The rate of the reaction is governed by the rate of diffusion of dissolved oxygen or cyanide to the surface of the gold, depending on their relative concentrations. Air (21% oxygen) is sufficient for the reaction to occur, but it was shown that using oxygen instead resulted in faster reaction rates [2]. Small amounts of sodium

hydroxide (about 0.01%) are also added to the cyanide solution to prevent the cyanide from hydrolysing to HCN, but sodium hydroxide retards the dissolution of gold by cyanide somewhat, so large quantities should be avoided [1,11].

Reaction rates for gold dissolution in cyanide solutions were compared at various temperatures, namely, 20°, 60° and 80°C. The optimum temperature was at 60°C. The slower dissolution at higher temperatures is probably due to the lower solubility of oxygen in solution [2].

Passivation of the gold surface can occur which slows down the rate of dissolution of gold in cyanide. It has been shown that the presence of small amounts of thallium almost eliminated passivation and accelerated the dissolution of gold about 7-fold [11].

The $[Au(CN)_2]^-$ complex can be electrolysed to form gold metal from an alkaline solution as follows:

$$4[Au(CN)_2]^- + 4OH^- = 4Au + 8CN^- + O_2 + 2H_2O$$

In practice, the liberated oxygen oxidises considerable cyanide to cyanate and carbonate [1].

7.2) ARSENIC

Arsenic has oxidation states of –3, 0, 3 and 5 of which the main ones are 3 and 5 [12]. Arsenic (III) is electrochemically active whereas arsenic (V) is not [12-14]. Arsenic (V) is thus reduced to arsenic (III) when total arsenic needs to be determined electrochemically. This has been done by using various reductants including sulphur dioxide [12,14,15], sodium sulphite [13,16,17], hydrazine [13,18-20], cuprous chloride [13,14,21], potassium iodide [13], ascorbic acid with potassium iodide [22], potassium bromide [18], hydroxylamine hydrochloride [13] and L-cysteine [23,24]. When making up the standard arsenic (III) solutions, reductants such as hydrazine chloride [12,18] or ascorbic acid [14] were added to ensure that none of the arsenic was oxidised; however, it was not found necessary. It is important that the reductants ensure rapid quantitative conversion to arsenic (III) and that any excess or by-products do not interfere with the determination. It was found that small amounts of

hydrazinium chloride raised the background current, and the gold film electrode became tarnished when sulphur dioxide was used, probably due to the formation of gold sulphite [12]. Davis *et al.* [21] used a process called reductillation which first involved reduction with cuprous chloride and then the distillation of arsenic (III) to get rid of interference. Arsenic (V) has been directly determined on a heated gold microelectrode where the high temperature increases the reaction rate of the sluggish reduction process [25]. It was also shown that arsenic (V) becomes electroactive in the presence of mannitol [26].

7.3) BACKGROUND

It was decided not to separate of the arsenic from the gold as minimal sample manipulation is preferred for trace analysis. Instead the kinetically inert gold (I) cyanide complex was formed. In this work potassium aurous cyanide ($K[Au(CN)_2]$) was used instead of dissolving the gold in the manner proposed earlier. This offered more controlled conditions as the impurities could be added as needed. Sodium cyanide was added to the solution to make up for any excess cyanide after the gold dissolution. A concentration of 10^{-3} $mol.l^{-1}$ cyanide was used which should have been sufficient to account for the actual excess. Arsenic was added in the form of arsenic (III) oxide (As_2O_3) which was dissolved in a basic solution. Arsenic (III) oxidation is accelerated by acidification, so this was avoided [31].

A suggested method for the dissolution of gold is, however, proposed. Use finely divided gold to increase the dissolution rate if possible. Add a solution of 0.1% (m/v) KCN and 0.01% (m/v) KOH. Heat to 60°C while stirring. Sparging air or oxygen into the solution will also speed up the reaction, but gas flow rates should not be too high or else evaporation or volatilisation could occur. The resultant solution should contain some excess cyanide and the $K[Au(CN)_2]$ complex should have formed.

The initial work was done in a normal cell in the BAS C2 Cell Stand. This acted as a Faraday cage. Once matrix exchange was implemented, the flow system was utilised.

7.4) EXPERIMENTAL AND RESULTS

7.4.1) pH of Plating Solution

Initially cyclic voltammetry (CV) was done for the various solutions to assess the system and to ascertain where the oxidation and reduction peaks were situated. The starting point was to establish whether the gold (I) cyanide complex and the free cyanide oxidation peaks would interfere with that for arsenic. All these voltammograms were run at a scan rate of 20 $mV.s^{-1}$ with an initial negative-going scan. Various pH values were considered, beginning with a pH of 9, which was achieved by the addition of sodium hydroxide. The cyclic voltammograms for cyanide, arsenic + cyanide and gold (I) cyanide + cyanide, where the cyanide concentration in each case was 10^{-3} $mol.l^{-1}$, are shown in figure 7.1. The cyanide does not have an oxidation peak in the potential region looked at, but the gold (I) cyanide does produce peaks overlapping with the arsenic peak.

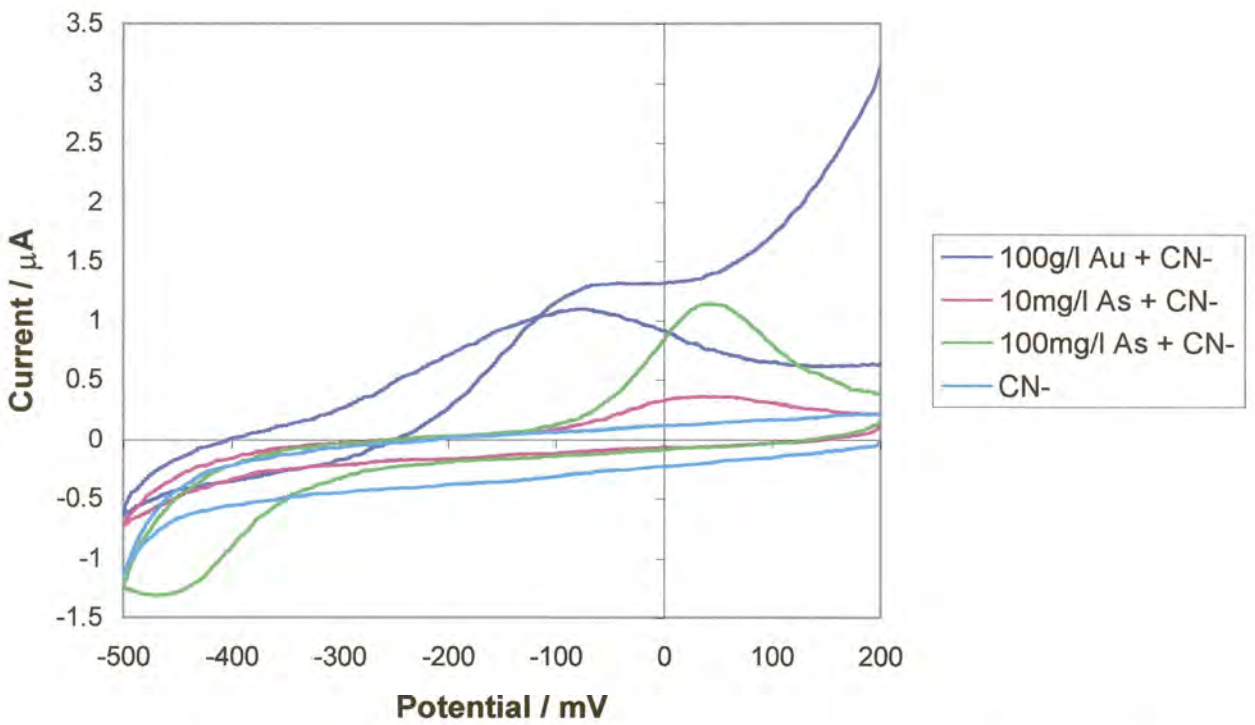

Figure 7.1: The cyclic voltammograms for cyanide, arsenic + cyanide and gold (I) cyanide + cyanide at a pH of 9

It was decided to investigate the effect of a slightly acidic solution at pH 4. In an acidic solution, arsenic (III) exists as the meta-arsenious acid, $HAsO_2$ and the electrochemical process is as follows [27]:

$$HAsO_2 + 3H^+ + 3e^- = As + 2H_2O \qquad E^\circ = +240 \text{ mV}$$

Above a pH of 8, the meta-arsenious acid dissociates to form the arsenite ion, AsO_2^- and the electrochemical process is as follows [27,28]:

$$AsO_2^- + 2H_2O + 3e^- = As + 4OH^- \qquad E^\circ = -680 \text{ mV}$$

Arsenic crystallisation then occurred at the electrode as follows [28]:

$$4As \rightarrow As_4$$

$$nAs_4 \rightarrow (As_4)_n$$

Arsenic dissolves from the electrode into both acidic or alkaline solution [10]. During anodic dissolution, the arsenic passes into solution as the trivalent state, As^{3+} [28].

The pH of solutions similar to those above, was adjusted to 4 by the addition of citric acid. The cyclic voltammograms are shown in figure 7.2. Once again the cyanide does not have an oxidation peak in the potential region studied. In the acidic solution, the gold (I) cyanide had a small peak more anodic than that for arsenic, thus no overlapping occurred. The arsenic peak shifted cathodic by less than 100 mV when moving from a pH 9 to a pH 4 solution. According to Bard [28], the potential for the reversible electrode process for the As/As_2O_3 system depends on the pH according to the following relationship which stems from the Nernst equation:

$$E = 0.234 - 0.059 \text{ pH}$$

The system is reversible from pH 3 to 10 in the absence of air. According to this, the potential at a pH of 9 should be –0.297 V and at a pH of 4 it should be 0.002 V. This implies that a shift of about 300 mV should. This was not observed in this system.

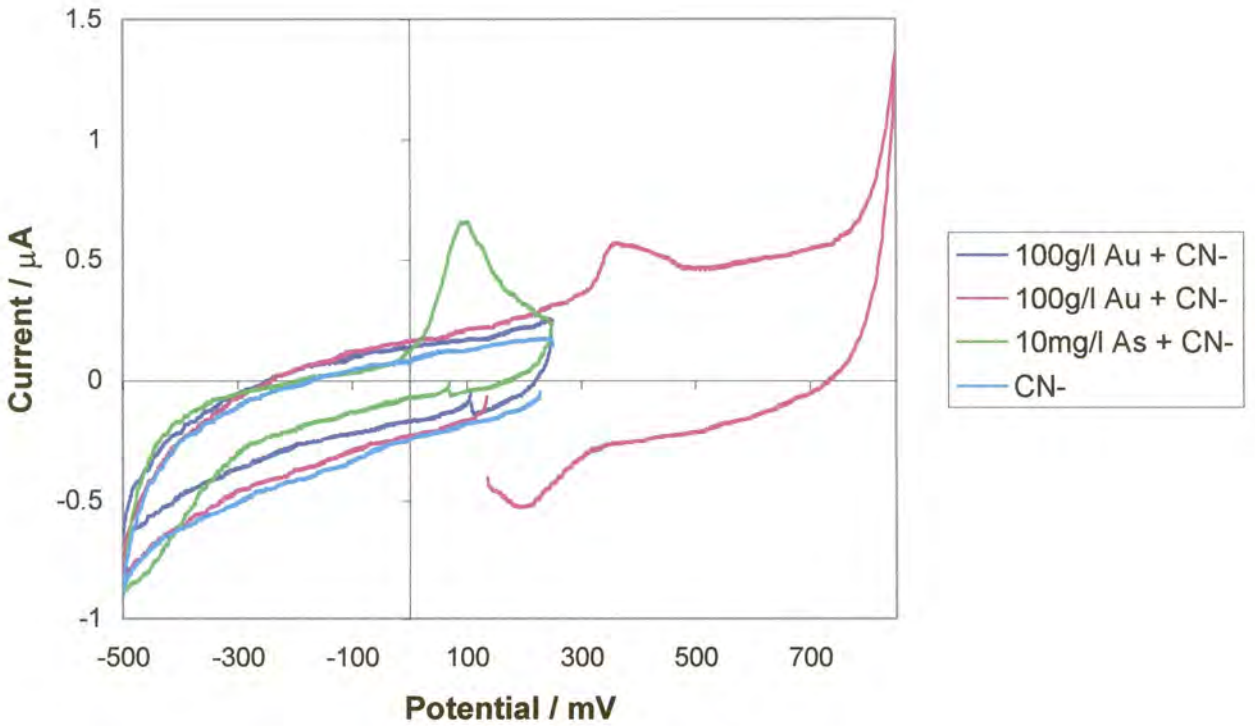

Figure 7.2: The cyclic voltammograms for cyanide, arsenic + cyanide and gold (I) cyanide + cyanide at a pH of 4

An arsenic solution containing cyanide at pH 8 was looked at. The cyclic voltammogram is shown in figure 7.3. The arsenic peak was very broad. Bard [28] pointed out that the compounds of arsenic (III) generate distinctive reduction waves whose nature to a large extent depends on the pH of the solution. In a neutral non-buffered solution, one extended or two closely spaced waves were observed. This was probably the extended peak that is seen in the voltammogram below. Also, when working in a neutral medium As_2O_3 is formed on anodic dissolution as follows:

$$2As + 3H_2O \rightarrow As_2O_3 + 6H^+ + 3e^-.$$

The As_2O_3 will accumulate at the electrode surface and inhibit the anodic dissolution as it is poorly soluble in a neutral solution [28]. It was thus best to avoid neutral or near neutral solutions for this determination.

It was decided to add a supporting electrolyte to improve the conductivity of the solution. KNO_3 was added for this purpose such that the concentration was 0.1 $mol.l^{-1}$. This reduced the iR drop significantly to acceptable levels. This component was added to all solutions from here onward.

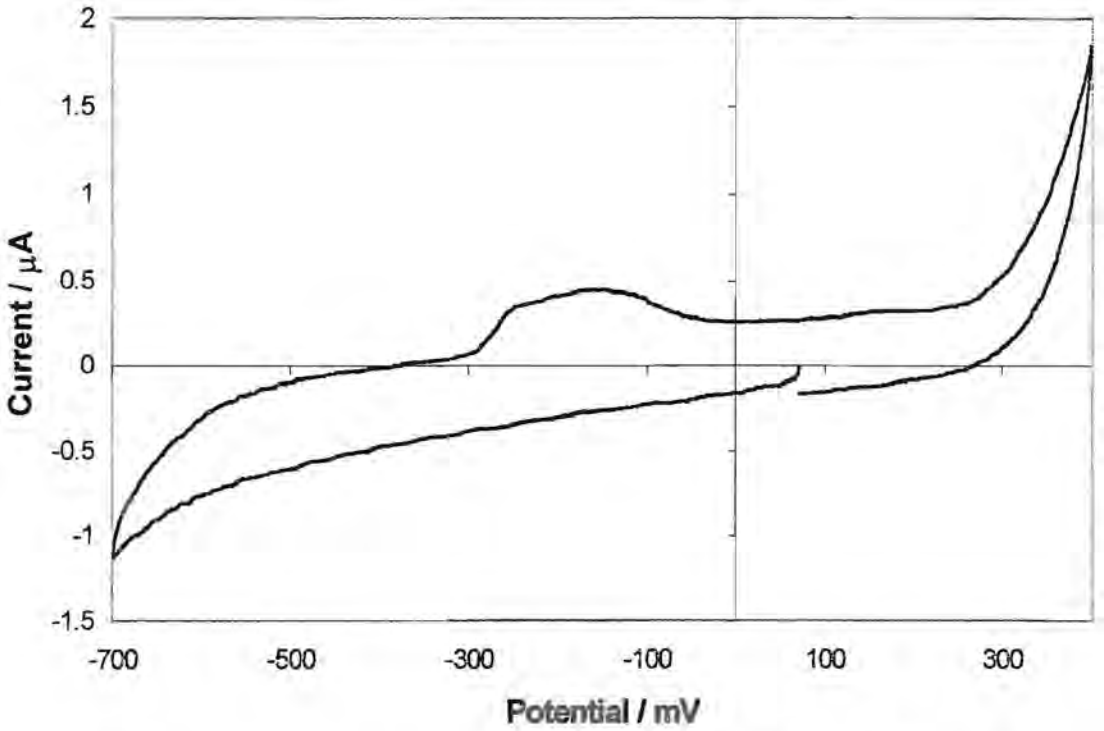

Figure 7.3: The cyclic voltammogram for 100 $mg.l^{-1}$ arsenic + 10^{-3} $mol.l^{-1}$ cyanide at a pH of 8

When working with an arsenic + cyanide solution at pH 10, it was noted that the first run, which was done on a newly formed gold film, showed some kind of peak. However, on the second run, done straight after the first, the peak had disappeared. The cyclic voltammograms are displayed in figure 7.4. The rest potential also became progressively more positive after each run. A similar result was obtained for solutions at pH 11 and 12, where the arsenic peak disappeared or became less sensitive for successive runs. This indicated that the electrode was being passivated under these alkaline conditions.

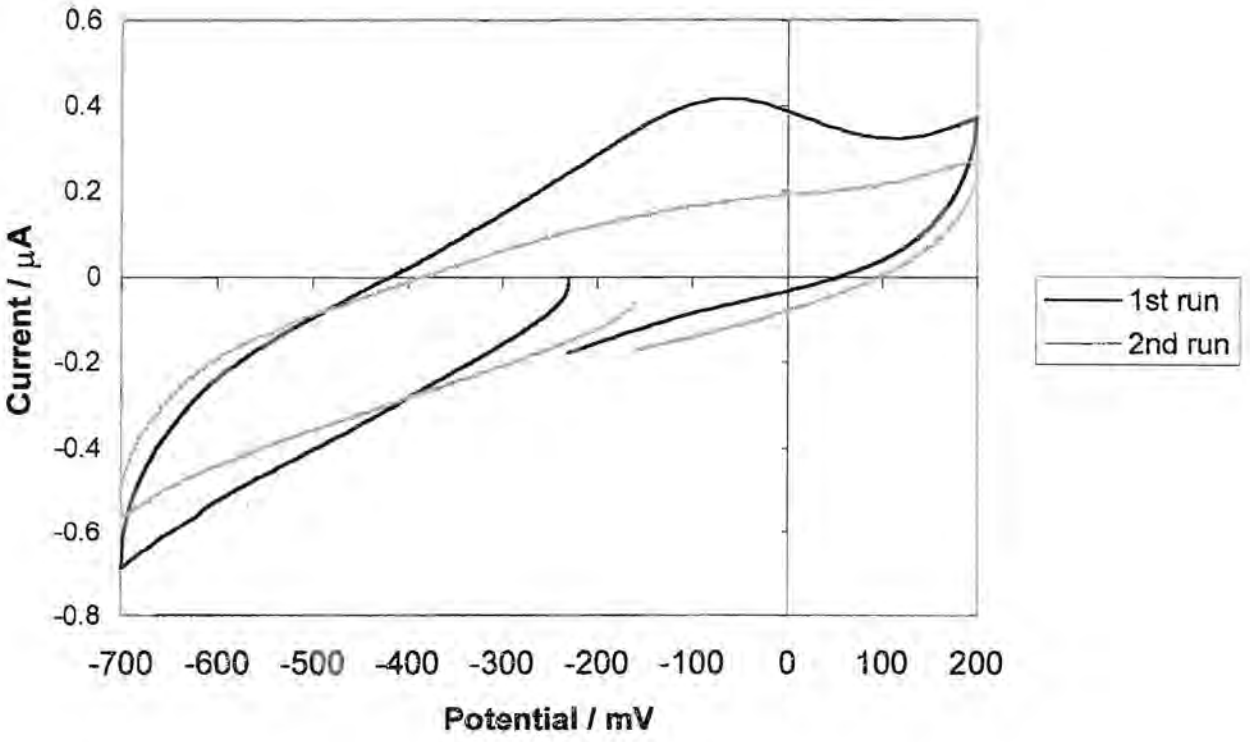

Figure 7.4: The cyclic voltammograms for 100 mg.l^{-1} arsenic + 10^{-3} mol.l^{-1} cyanide at a pH of 10

The two components that could have been responsible for the electrode passivation would be the arsenic or the cyanide. The arsenic concentration was reduced to 10 mg.l^{-1}, but the same trend arose. Two solutions were prepared at a pH of 12: the first contained 10 mg.l^{-1} arsenic + 10^{-3} mol.l^{-1} cyanide and the second only contained 10 mg.l^{-1} arsenic (both of which contained the 0.1 mol.l^{-1} KNO_3). The cyclic voltammograms produced are presented in figure 7.5.

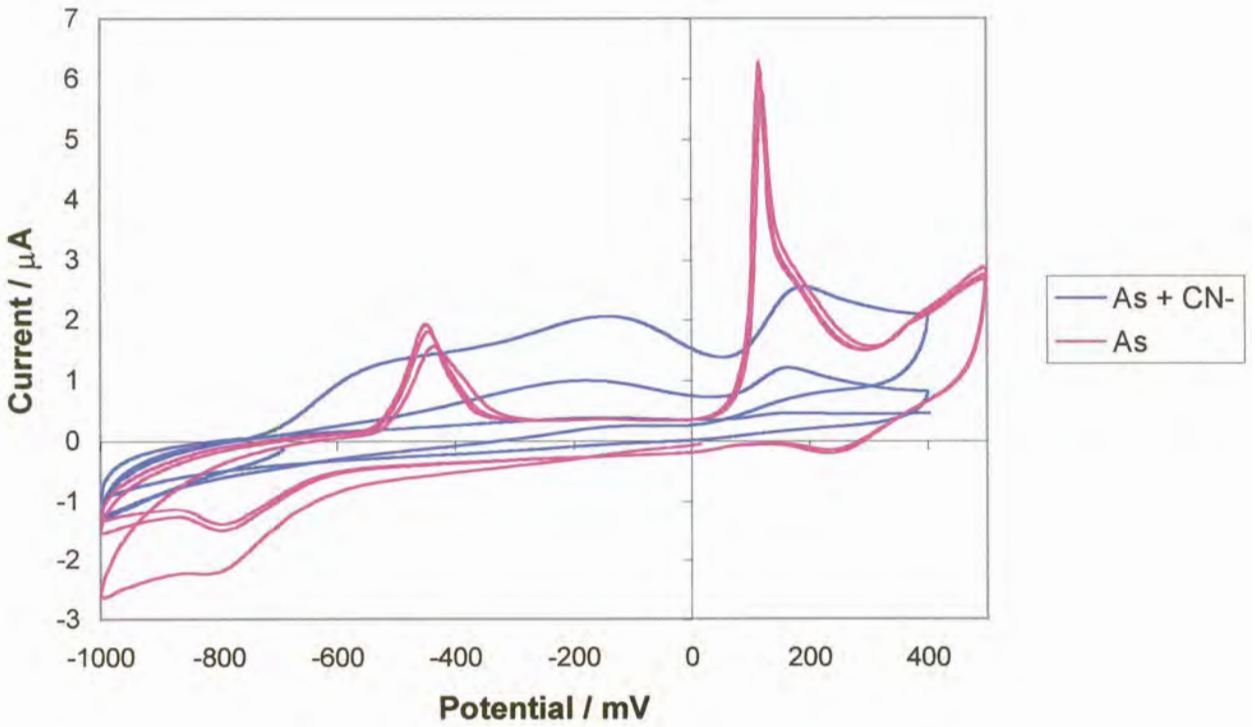

Figure 7.5: The cyclic voltammograms for 10 mg.l^{-1} arsenic + 10^{-3} mol.l^{-1} cyanide and 10 mg.l^{-1} arsenic only at pH 12

A definite passivation of the gold film electrode was observed for the solution containing both arsenic and cyanide. However, the solution containing only arsenic exhibited fairly reproducible results for the successive scans. This pointed to the cyanide being responsible for the passivation effect. This was also found in the leaching of gold from ore, where a passivated gold film could form in the presence of oxygen, cyanide and hydroxide [32]. The voltammograms also showed how the presence of cyanide shifted the arsenic peak potential to more positive values.

The peak at about –440 mV in the absence of cyanide corresponded to the arsenic (III) peak used by Aldstadt *et al.* [27] as shown in figure 7.6. This was also determined in a sodium hydroxide solution at a pH of 12. Bard [28] noted that on moving from a neutral to an alkaline solution, the first wave disappears and the remaining peak shifts to the cathodic region. This too was observed in this work.

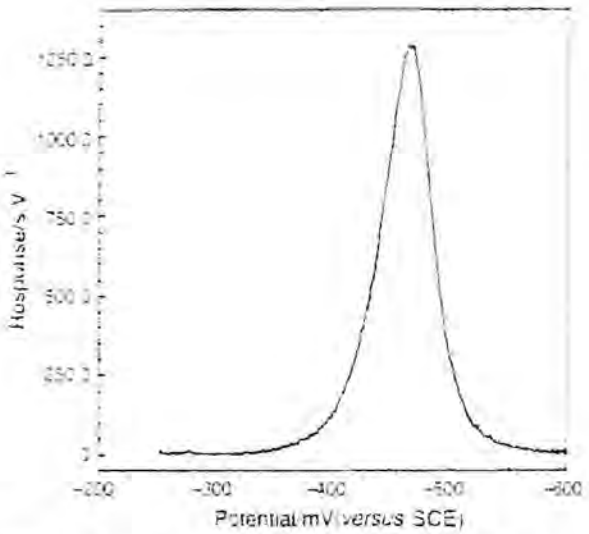

Figure 7.6: The arsenic (III) signal found by Aldstadt *et al.* [27]

Even though using a basic solution to determine arsenic (III) has the advantage of reducing the effects of interfering metals [27], as these would precipitate at high pH values, acidic solutions needed to be considered. The uncomplexed cyanide present in alkaline solutions passivated the gold film electrode which would have resulted in a new gold film having to be formed between each analysis. This would have been tedious and would have resulted in less reproducible results. Also there would be no interference from the gold (I) cyanide.

The sodium cyanide added to the solution should totally dissociate, producing "free" cyanide, CN^-. This would be the uncomplexed cyanide. The CN^- reacts with water to form hydrocyanic acid, HCN. The formation constant is 4.93×10^{-10} [11]. In other words:

$$K_a = \frac{[CN^-][H^+]}{[HCN]}$$

$$K_a = 4.93 \times 10^{-10}$$

Therefore in a solution at pH 12, all the cyanide would be present as CN^- and at pH 3, almost all the cyanide would be present as HCN. HCN is soluble in water giving a weak acid solution. Thus in an acidic solution, there would be very little CN^- to react with the gold film. A pH below 3 could not be considered as the $[Au(CN)_2]^-$ complex would decompose to form AuCN which precipitates under more acidic conditions [33-35].

A 10 $mg.l^{-1}$ arsenic solution was made up as before, containing NaCN and KNO_3, and then the pH was adjusted to 3 by the addition of citric acid. Arsenic (III) oxidation is accelerated by acidification [34], therefore it is important to analyse the samples soon after they have been acidified. The cyclic voltammograms in figure 7.7 showed that no passivation of the gold film occurred at this pH, in both a quiescent and a stirred solution.

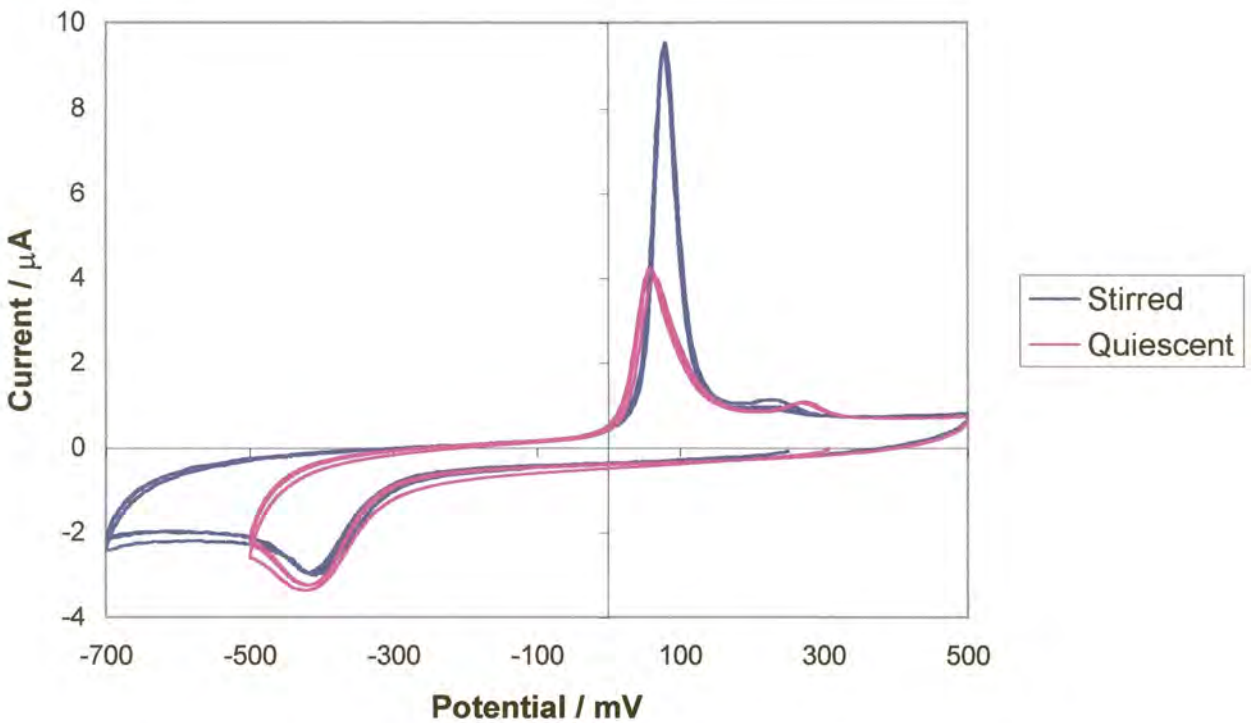

Figure 7.7: Cyclic voltammograms for 10 $mg.l^{-1}$ arsenic (III) + 10^{-3} $mol.l^{-1}$ cyanide at pH 3

The small peak at about 230 mV (in the stirred solution) may have been due to some impurity in the gold that made up the gold film. It was observed that the unknown peak vanished after a number of runs, as shown in figure 7.8, but reappeared once a new film was plated. There was also a slight loss in sensitivity for the arsenic peak, but not sufficient to account for the disappearance of the unknown peak. The change in the arsenic (III) reduction potential indicated that the properties of the gold film were changing. This could have been due to the impurity being stripped from the film. The unknown peak fading faster in the stirred solutions than in the quiescent solutions reinforced this. In the stirred solution the impurity would be rapidly swept away and hence removed from the vicinity of the electrode surface. This would

prevent the impurity from being reduced onto the electrode surface again. In a quiescent solution, the main mass transport process moving the impurity away from the electrode surface would be diffusion, which is a much slower process. Some of the impurity could therefore be redeposited onto the electrode surface, and hence the peak would diminish at a slower rate.

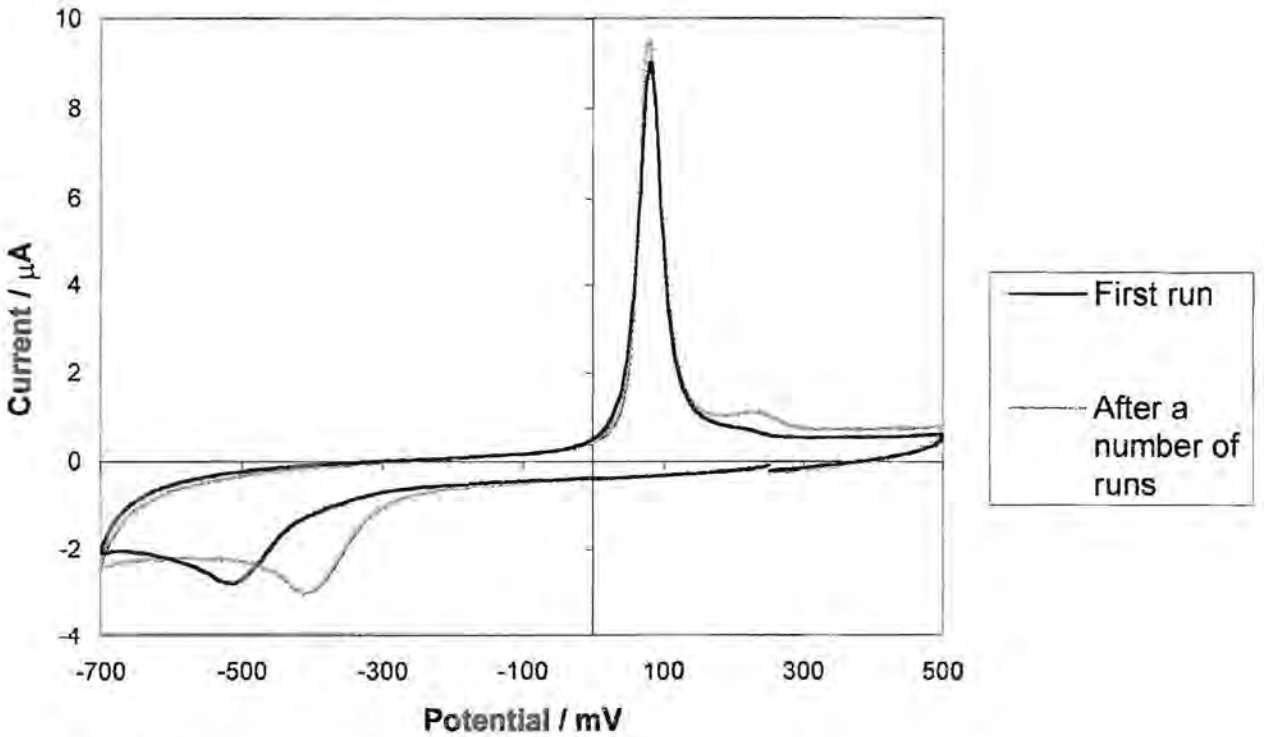

Figure 7.8: Cyclic voltammograms showing the disappearance of the unknown peak for a stirred solution after a number of runs

A solution containing 10 $g.l^{-1}$ gold, present as $[Au(CN)_2]^-$, was made up with 10 $mg.l^{-1}$ arsenic (III), 10^{-3} $mol.l^{-1}$ cyanide and 0.1 $mol.l^{-1}$ KNO_3 adjusted to pH 3 with citric acid. A cyclic voltammogram was again run to establish whether the gold would interfere with the arsenic and also to ensure that the gold (I) cyanide complex had not broken up at this pH. Figure 7.9 reveals that the gold (I) cyanide complex is still intact and that a 1000-fold more gold than arsenic did not interfere with the arsenic determination at all. There was also scope to increase the gold to arsenic concentration ratio without any difficulties being experienced.

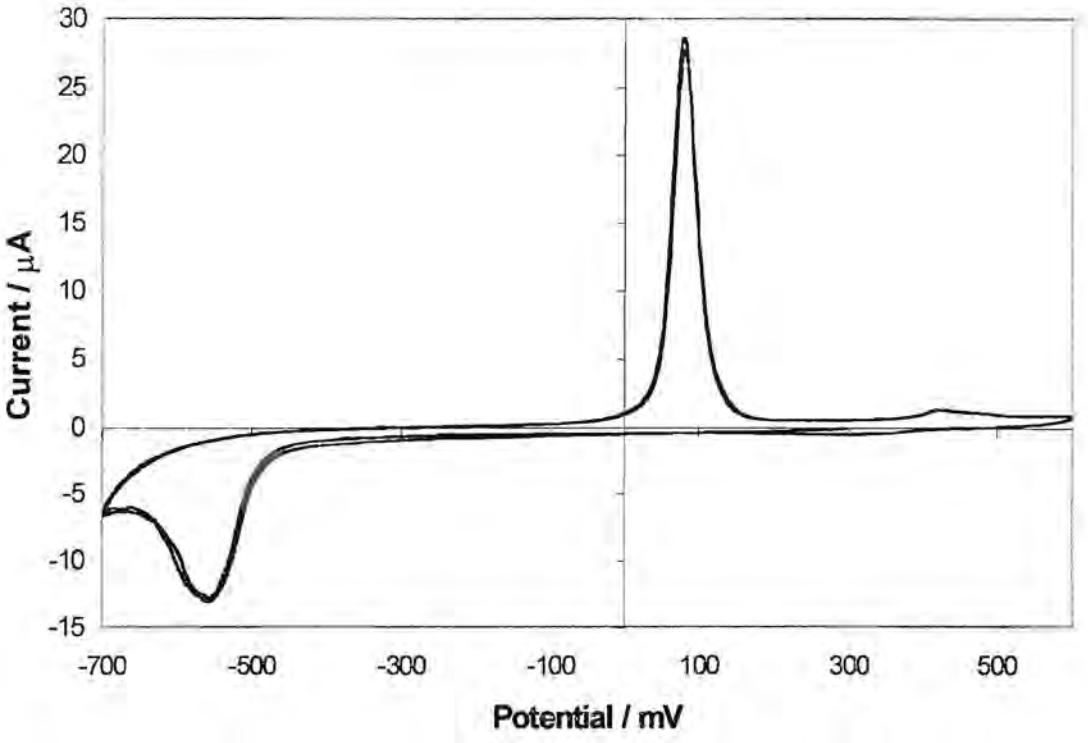

Figure 7.9: Cyclic voltammogram for 10 $g.l^{-1}$ gold (as $[Au(CN)_2]^-$) + 10 $mg.l^{-1}$ arsenic(III) + 10^{-3} $mol.l^{-1}$ cyanide at pH 3

Other important information could also be gained from the cyclic voltammograms [36]. The system that was to be studied further, displayed in figure 7.9, was looked at in more detail. For a chemically and electrochemically reversible couple,

$$\Delta E_p = E_{pa} - E_{pc} \approx \frac{0.058}{n}$$

In this case the arsenic redox reaction was a three electron process, therefore:

$$\Delta E_p \approx 0.019\,V$$

However, when looking at the peak separations,

$$\Delta E_p = 0.08 - (-0.58)$$

$$\Delta E_p = 0.59\,V$$

This implied that the arsenic redox system was irreversible and that the electron transfer between the electrode and the arsenic was slow. Also, for a reversible couple with no kinetic complications,

$$i_{pa} \approx i_{pc}$$

This was not the case for either a quiescent or a stirred solution.

7.4.2) Deposition Potential

The optimum deposition potential for arsenic (III) in a solution at pH 3 was investigated. The gold (I) cyanide complex was omitted from most of the solutions, unless specified otherwise, due to the cost of the substance as it was already proven that it would not interfere with the arsenic determination. A 10 $mg.l^{-1}$ arsenic (III) solution was made up as before. LSSV was done at various deposition potentials in a stirred solution with a deposition time of 10 s and a scan rate of 20 $mV.s^{-1}$. The results displayed in figure 7.10 show that the optimum deposition potential was –650 mV. This potential was used from here onward.

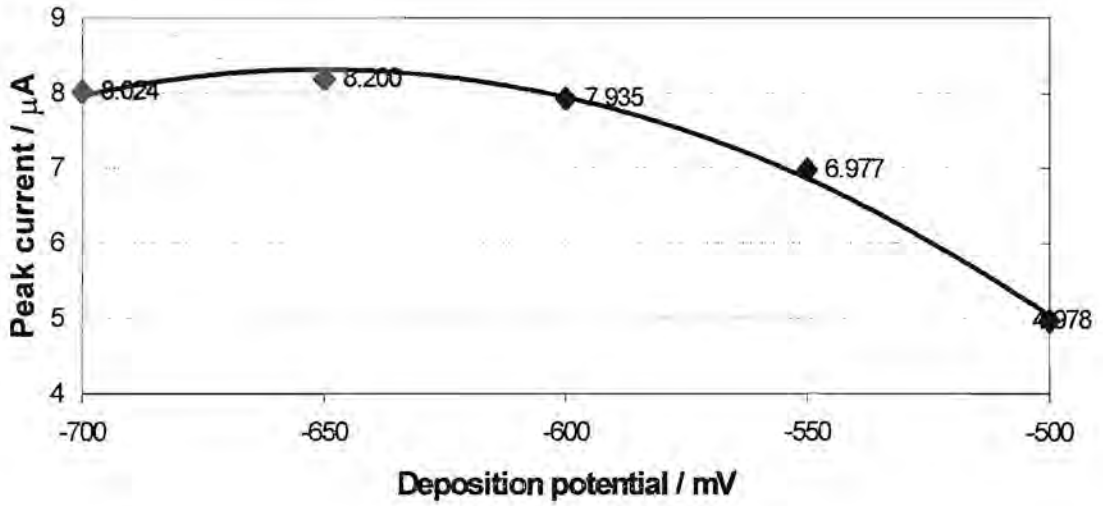

Figure 7.10: Graph of peak current versus deposition potential

7.4.3) Reproducibility

The reproducibility of the system was investigated by doing 10 runs of LSSV as above. This produced a RSD of 4.4%. This is acceptable, but there were some concerns. The peak current showed a definite increasing trend. This could be due to not all the arsenic being stripped from the electrode and hence a slow accumulation of arsenic. Also, the peak potential moved towards low values with successive runs. This seems to indicate that there is a slow change in the electrode surface.

7.4.4) Stripping Electrolytes

It was decided to look at a matrix exchange method to see whether it would be possible to reduce the gold film degradation. This would also help to improve the sensitivity of the determination and reduce interference. The flow system described in chapter 5 was used with deoxygenation taking place. iR compensation was always used.

7.4.4.1) Hydrochloric Acid

Hydrochloric acid was the first stripping electrolyte investigated as it was widely used and provided good sensitivity. The stripping peaks were also narrow which indicated that the charge-transfer reaction was fast and reversible [12,21,30]. It was found that when arsenic was determined in a hydrochloric acid matrix, chlorine was generated at the auxiliary electrode concurrent with arsenic deposition at the working electrode. The chlorine would then diffuse to the working electrode where it would readily oxidise the gold electrode surface, thereby making it inactive [27]. This was not a problem when using a WJE as only the solution from the jet reached the electrode surface, thus the chlorine could not diffuse to the working electrode and attack it. It has also been postulated that the gold film was oxidised in the presence of a high chloride concentration to the $[AuCl_4]^-$ complex. This would lead to the active gold surface area decreasing and hence poor reproducibility [12]. It was, however, suggested that hydrochloric acid concentrations greater than 7 $mol.l^{-1}$ be avoided as it could lead to the destruction of the glassy carbon substrate on prolonged exposure [29].

Various hydrochloric acid concentrations were considered and the corresponding peak currents were measured to determine which concentration gave the best sensitivity. This was done in the wall-jet flow cell using the FlowTEK procedure previously depicted in figure 5.26. The plating solution was a 1 $mg.l^{-1}$ arsenic (III) solution containing 10^{-3} $mol.l^{-1}$ cyanide and 0.1 $mol.l^{-1}$ KNO_3 adjusted to pH 3 using a citrate buffer. The citrate buffer was made up by mixing 0.1 $mol.l^{-1}$ disodium citrate with 0.1 $mol.l^{-1}$ hydrochloric acid in a ratio of 39.9 to 60.1. The disodium citrate was made up by adding

2.1014 g citric acid monohydrate to 20 ml 1 mol.l^{-1} sodium hydroxide and making it up to 100 ml. The buffer was then diluted 10 times when added to the sample. The buffer was used instead of just citric acid as it could control the pH more accurately. Data were collected using DPSV from –400 mV to 300 mV at a scan rate of 20 mV.s^{-1} after a 20 s deposition time at –650 mV. The other parameters were the default parameters of 50 mV pulse amplitude, 50 ms pulse width, 20 ms sample width, and 200 ms pulse period.

The results are displayed in figure 7.11. A 4 mol.l^{-1} hydrochloric acid concentration was used in further studies as it gave the best sensitivity. Higher hydrochloric acid solutions were not considered to prevent any degradation of the working electrode.

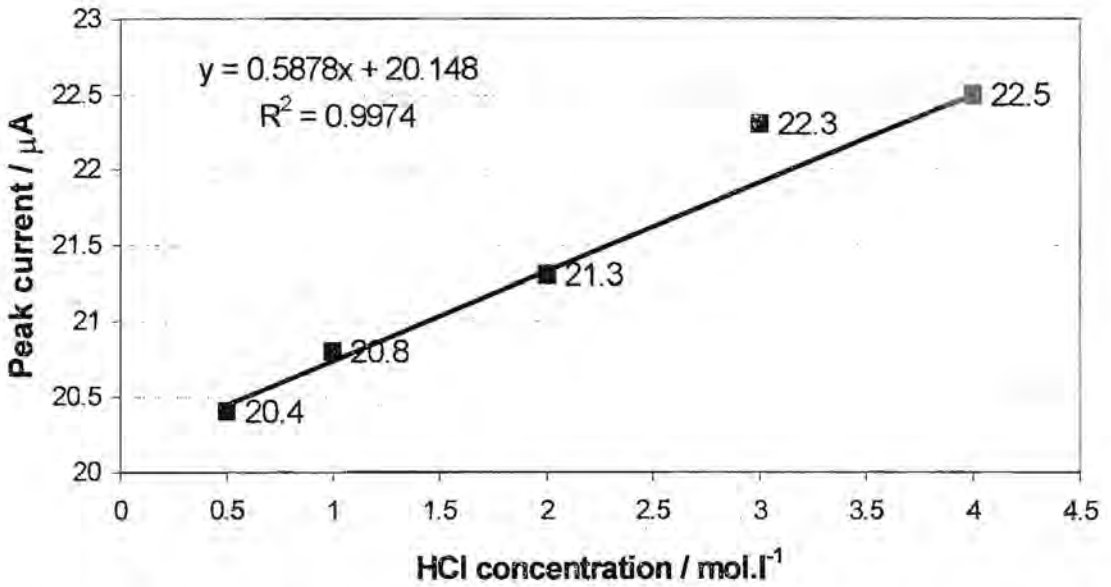

Figure 7.11: Graph of peak current versus hydrochloric acid concentration of the stripping electrolyte

A range of arsenic concentrations from 0.1 mg.l^{-1} to 1 mg.l^{-1} were studied to determine whether the relationship between arsenic concentration and peak current is linear. Data were collected using DPSV from –200 mV to 300 mV at a scan rate of 20 mV.s^{-1} after a 60 s deposition time at –650 mV. The other parameters were the default parameters as above. The FlowTEK method used was shown in figure 5.27.

Initially, instead of analysing the samples in an order of increasing concentration, the samples were mixed up and the 1 $mg.l^{-1}$ and 0.1 $mg.l^{-1}$ samples were transposed when analysed. The 1 $mg.l^{-1}$ arsenic solution was then analysed again. The findings are represented in figure 7.12. The peak current of 1.37 μA at 1 $mg.l^{-1}$ arsenic is the measurement taken again at the end of the analyses. This showed that the electrode definitely had some memory effects.

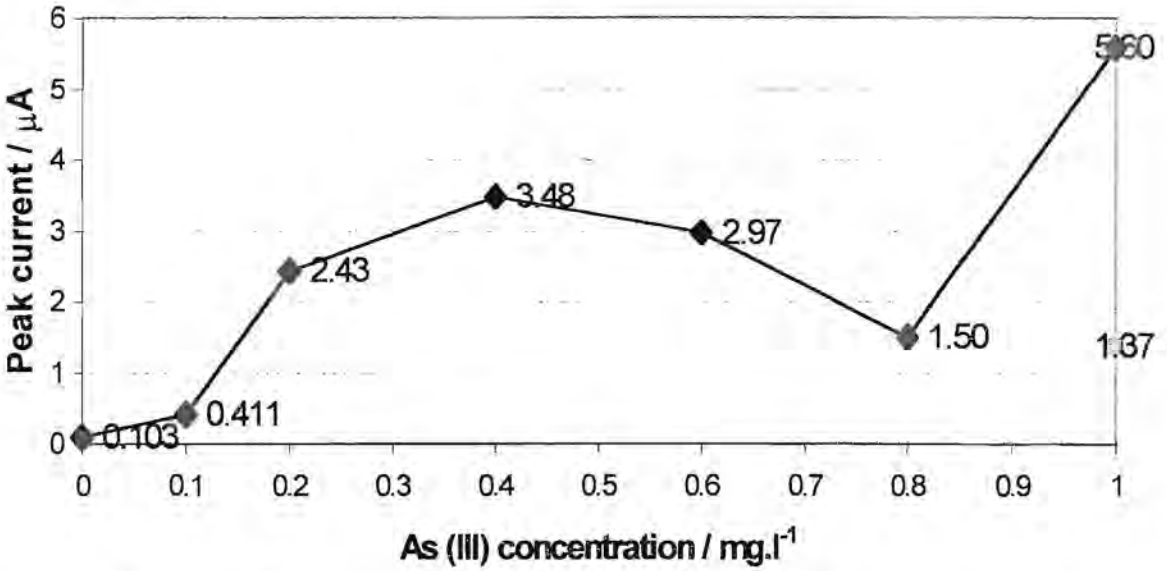

Figure 7.12: Graph of peak current versus arsenic (III) concentration where the order of analysis was not increasing in concentration

The experiment was repeated, but this time the samples were analysed in order of increasing concentration. The results are depicted in figure 7.13 and the voltammograms are shown in figure 7.14. The results were initially linear, but deviated from linearity after the 0.2 $mg.l^{-1}$ arsenic solution. This could have been due to the active surface area of the electrode being almost totally covered by arsenic (0). As elemental arsenic is a very poor conductor of electricity, only a monolayer of arsenic is deposited and therefore the peak current is limited [12,21,27,29,30]. A shorter accumulation time would solve this non-linearity at higher arsenic concentrations. Alternatively, it could have been that the gold film was degrading with time and the sensitivity started decreasing. This is quite possible as seen from the previous experiment

when the order of samples was confused, the gold film electrode was not very robust.

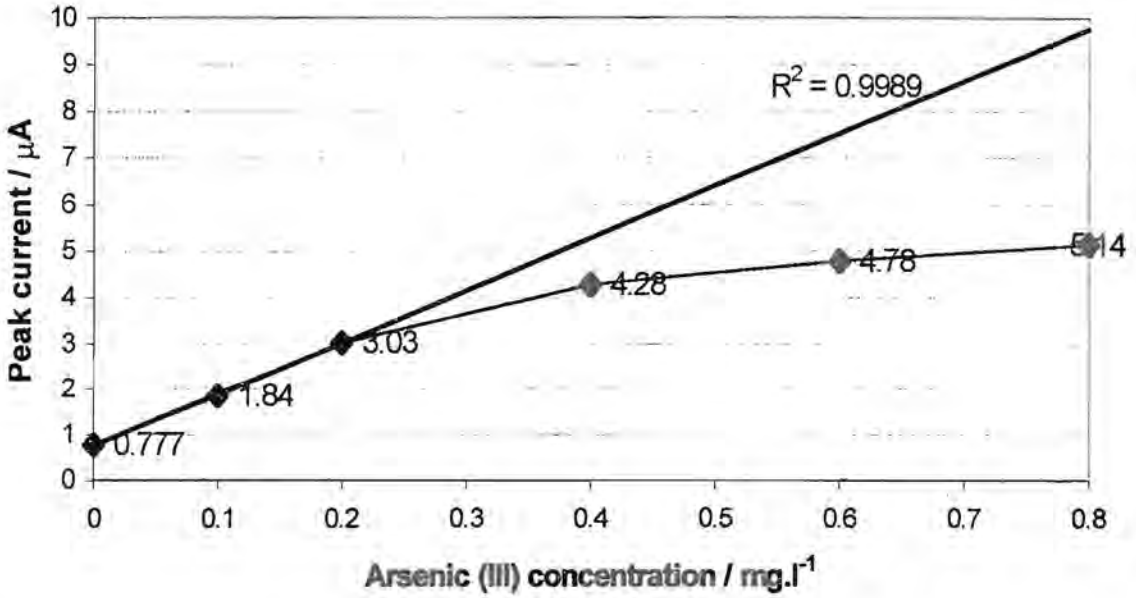

Figure 7.13: Graph of peak current versus arsenic (III) concentration where the order of analysis was increasing in concentration

It was therefore recommended that the samples should be read in order of increasing concentration. This would not be possible if data for a calibration graph were first collected and then the sample analysed, as the latter would probably give a deceptive lower current signal. Rather a method of standard addition could be used, which would not only make it possible to analyse in the concentration order required, but would also take the matrix effects into account.

The arsenic oxidation peaks were not symmetrical, particularly for the higher arsenic concentrations. There appeared to be a shoulder on the left side of the peaks. This could be due to the surface of the gold film changing with time, which supports the second postulate as to why the graph of arsenic concentration versus peak current deviated from linearity. It would be interesting to calculate the peak area and determine if it would yield more satisfactory results.

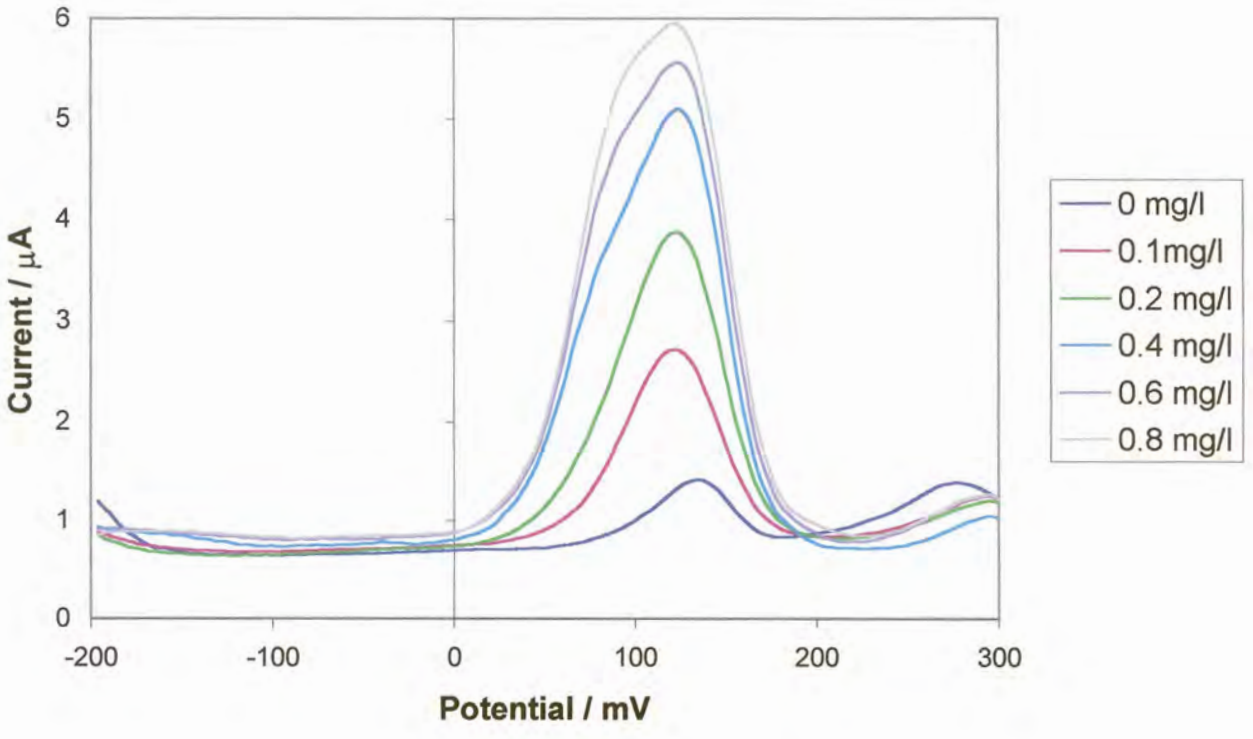

Figure 7.14: Voltammograms for increasing arsenic (III) concentration

7.4.4.2) Sulphuric and Hydrochloric Acid

Other stripping electrolytes were also investigated to find if the gold film electrode would degrade to a lesser extent.

At this point it was difficult to achieve a lustrous gold film of low resistance, so a step function was used to try and rejuvenate the glassy carbon electrode activity. The step function involved stepping from –1200 mV to 700 mV applying a pulse width of 250 ms for 1000 cycles in the gold plating solution. The gold film was then plated onto the GCE and it was found that this did improve the quality of the gold film.

A DPSV was collected for a 1 $mg.l^{-1}$ arsenic solution as before in the 4 $mol.l^{-1}$ hydrochloric acid solution. The voltammogram yielded a shoulder at about 180 mV that was not present before the electrochemical electrode treatment, as shown in figure 7.15. The shoulder decreased on successive runs while the main peak increased slightly. The origin of this shoulder is unknown. However, it could have been that with the electrochemical electrode

treatment, the electrode was activated to a greater degree which made conditions favourable for impurities to plate to a greater extent on the electrode. With successive runs, the impurity was stripped from the gold film which led to the reduction of the shoulder height. The arsenic peak could have increased in height as the impurity was stripped because a greater surface area of the electrode was now covered by gold.

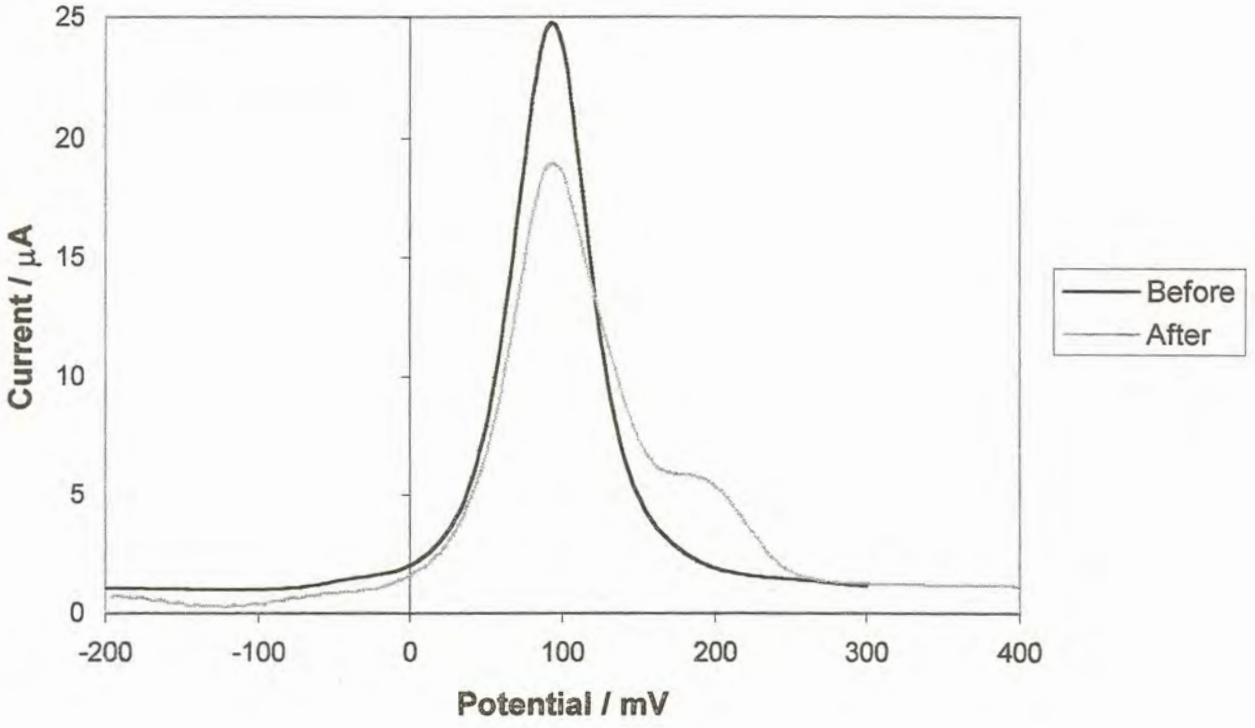

Figure 7.15: Voltammograms for 1 mg.l^{-1} arsenic with a 4 mol.l^{-1} HCl stripping electrolyte before and after electrochemical electrode treatment

Sulphuric acid as a stripping electrolyte was investigated. A 1 mol.l^{-1} solution produced a broad insensitive peak as shown in figure 7.16. 0.1 mol.l^{-1} hydrochloric acid was then added to this and it gave a sharper more sensitive peak. The shoulder that appears in the hydrochloric acid solution was resolved from the arsenic peak in the sulphuric acid-hydrochloric acid mixture. However the hydrochloric acid solution still yielded the most sensitive peak.

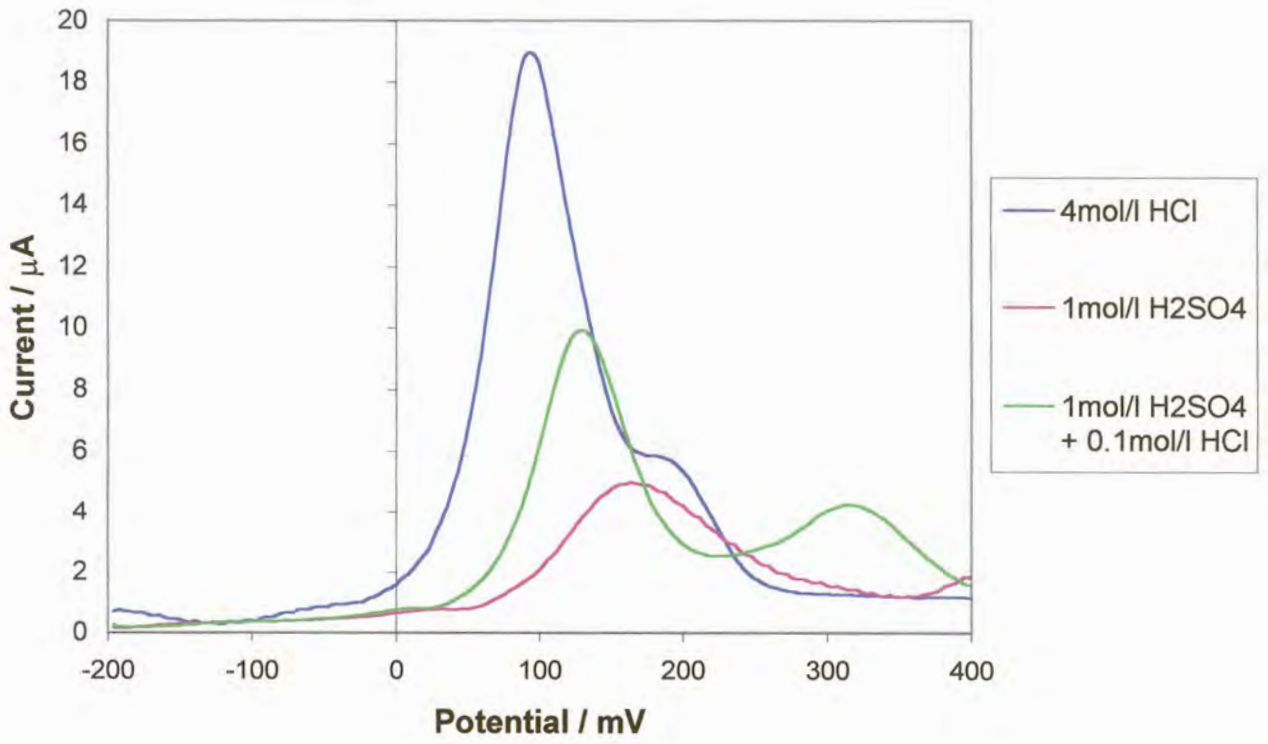

Figure 7.16: Voltammograms for 1 mg.l^{-1} arsenic with stripping electrolytes of 4 mol.l^{-1} HCl, 1 mol.l^{-1} H_2SO_4 and a mixture of 1 mol.l^{-1} H_2SO_4 + 0.1 mol.l^{-1} HCl

The sulphuric acid concentration was increased and the resultant voltammograms are presented in figure 7.17. The arsenic peaks were sharper and more sensitive for the 2 mol.l^{-1} sulphuric acid solutions containing hydrochloric acid than that for the 1 mol.l^{-1} solution. Increasing the amount of hydrochloric acid in the mixture also increases the peak height. Looking at even higher sulphuric acid concentrations did not alter the sensitivity significantly.

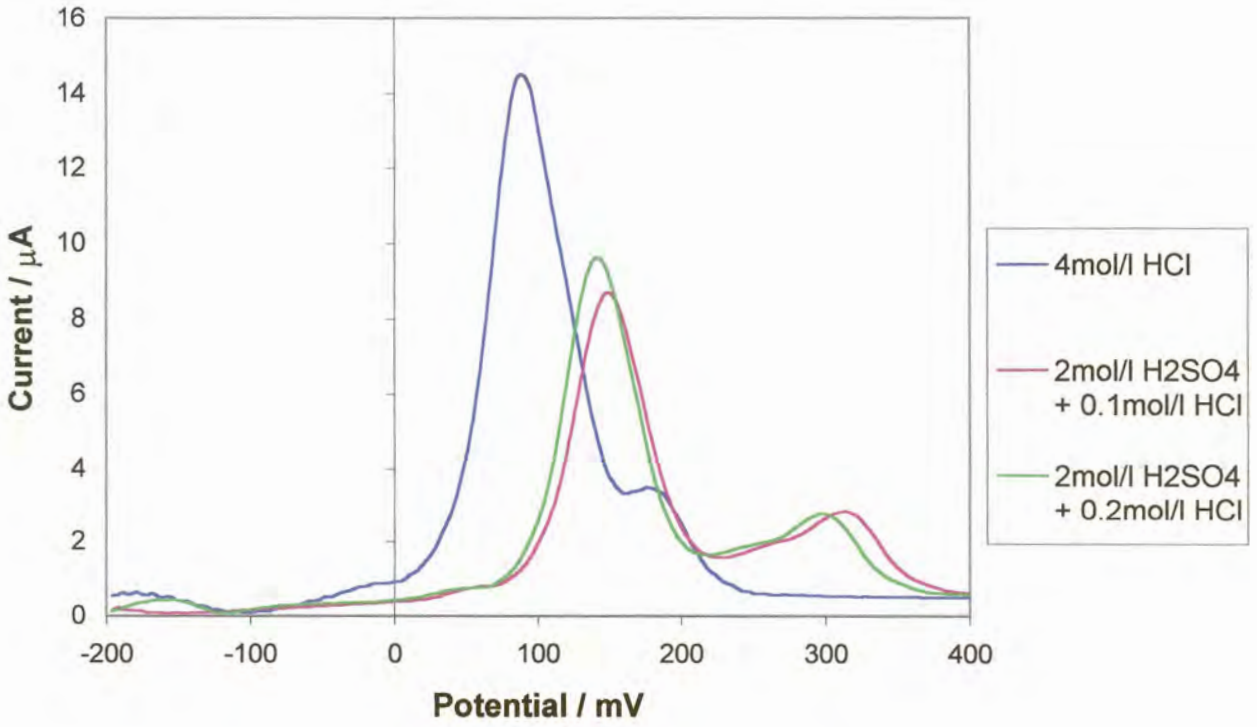

Figure 7.17: Voltammograms for 1 mg.l^{-1} arsenic with stripping electrolytes of 4 mol.l^{-1} HCl, 2 mol.l^{-1} H_2SO_4 + 0.1 mol.l^{-1} HCl and 2 mol.l^{-1} H_2SO_4 + 0.2 mol.l^{-1} HCl

The reproducibility for the two stripping electrolytes, that is 4 mol.l^{-1} hydrochloric acid and 2 mol.l^{-1} sulphuric acid + 0.2 mol.l^{-1} hydrochloric acid, was investigated. A 0.5 mg.l^{-1} arsenic solution was accumulated for 20 s at a potential of –650 mV. DPSV was performed between –200 mV and 400 mV at 20 mV.s^{-1}, with the other parameters being the default settings. The average peak height for the hydrochloric acid solution was 6.28 µA and the RSD was 3.2% for 20 runs. For the acid mixture, the average peak height was 3.30 µA with a RSD of 3.3%. The problem with the hydrochloric acid solution is that the position of the baseline had to be manually defined. This was due to the shoulder initially being well-defined and the baseline was drawn from the start of the peak to the start of the shoulder. With time the definition reduced and the baseline was then drawn from the start of the peak to the end of the shoulder.

The range of arsenic concentrations was again looked at using the 2 mol.l^{-1} sulphuric acid + 0.2 mol.l^{-1} hydrochloric acid stripping electrolyte. DPSV was applied from –200 mV to 400 mV at a scan rate of 20 mV.s^{-1} after a 60 s deposition time at –650 mV. The default settings were used for the other parameters. The results are depicted in figure 7.19 and the voltammograms are shown in figure 7.18. The correlation coefficient for the straight line was 0.9952 which shows greater linearity than that when using the 4 mol.l^{-1} hydrochloric acid as stripping electrolyte. This could be due to the reduced sensitivity when using the acid mixture. However, the polynomial fit to the calibration showed that there was a slight deviation from linearity.

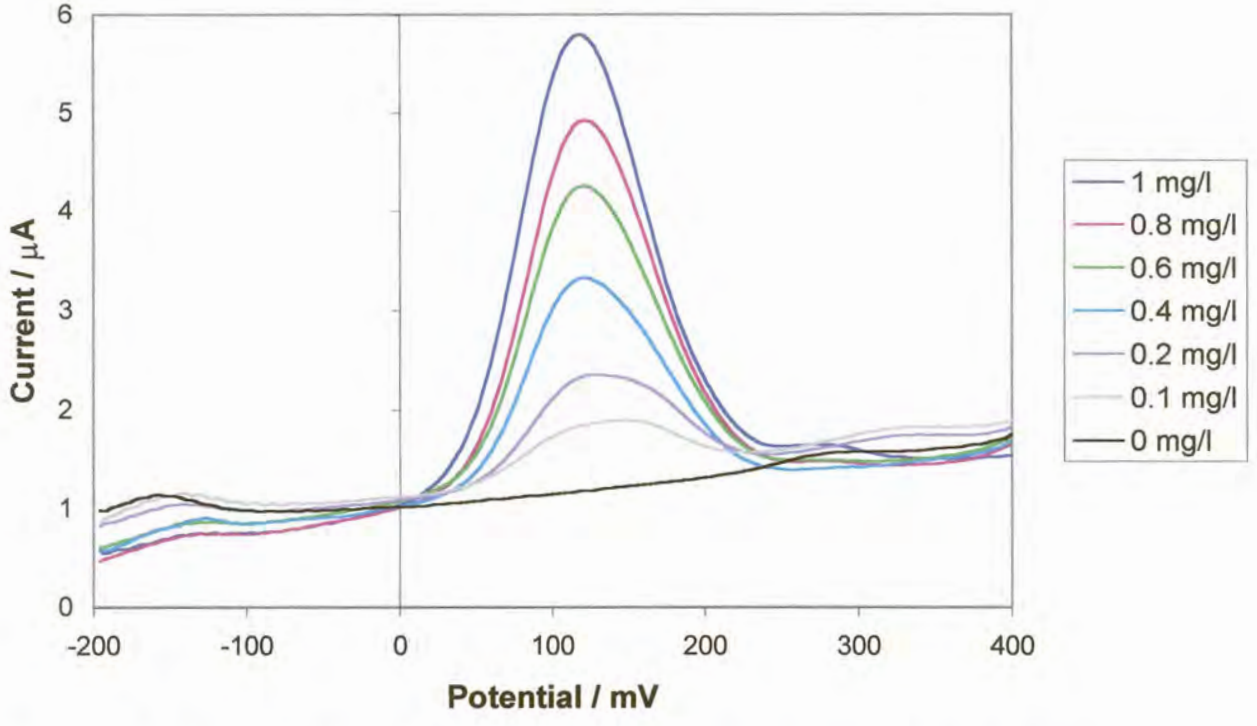

Figure 7.18: Voltammograms for increasing arsenic (III) concentration when using a 2 mol.l^{-1} H_2SO_4 + 0.2 mol.l^{-1} HCl stripping electrolyte

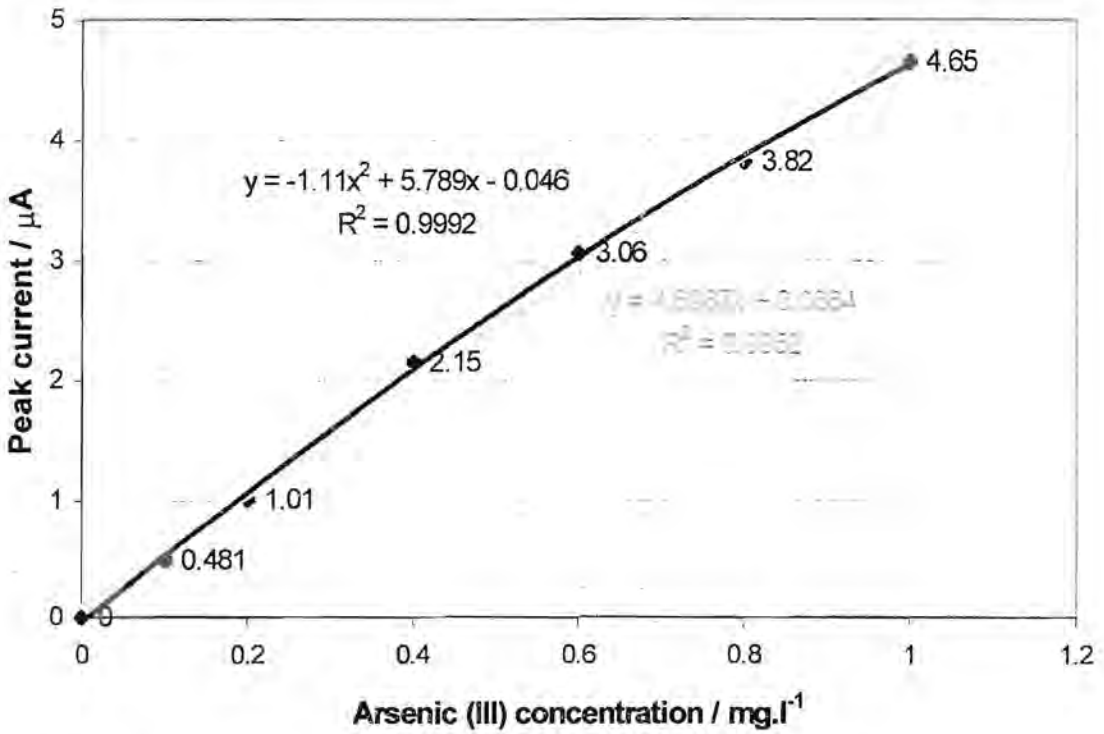

Figure 7.19: Graph of peak current versus arsenic (III) concentration when using a 2 mol.l^{-1} H_2SO_4 + 0.2 mol.l^{-1} HCl stripping electrolyte

It still remains difficult to say which stripping electrolyte is better to use, the 4 mol.l^{-1} hydrochloric acid solution or the 2 mol.l^{-1} sulphuric acid + 0.2 mol.l^{-1} hydrochloric acid solution. That would need to be assessed according to the requirements of the experiment.

7.4.3) Interferences

A list of impurites and their approximate concentrations in high purity gold was given in table 1.1. These impurities could also be possible interfents in the arsenic determination. In particular, copper, mercury, antimony, silver, selenium, bismuth and so on have been mentioned [12,13,16,29,31,35,36]. In this study, cobalt, silver and copper as interferences were investigated.

7.4.5.1) Cobalt

A 0.5 mg.l^{-1} arsenic solution was made up and data were collected as before, using a 20 s deposition time. The 2 mol.l^{-1} sulphuric acid + 0.2 mol.l^{-1} hydrochloric acid stripping electrolyte was used. Cobalt nitrate was added

such that the cobalt concentration was 0.5, 5 and 50 $mg.l^{-1}$ in the various solutions. The peak current for arsenic was monitored and compared to that with no cobalt present. The cobalt, at any of the concentrations, did not have an effect on the arsenic peak. Thus in the gold matrix that is being consider, cobalt should not present any problems.

7.4.5.2) Silver

Silver was added to the arsenic solutions as silver nitrate and was examined in the same manner as for the cobalt. At silver concentrations up to 5 $mg.l^{-1}$ there was no effect on the arsenic peak, but at 50 $mg.l^{-1}$ silver, the peak current for arsenic decreased. Interference at this level should not affect the analysis of arsenic in high purity gold due to the relatively low concentration of silver present in these samples.

7.4.5.3) Copper

The last interferent studied was copper. Once again it was added as its nitrate salt and analysed in a similar manner. However, the concentration range looked at was 0.2, 0.5, 1 and 5 $mg.l^{-1}$ copper. The voltammograms produced are given in figure 7.20. These show that concentrations above 0.2 $mg.l^{-1}$ seriously affect the arsenic peak due to the close proximity of these peaks to each other. By a 10 times excess of copper, the arsenic peak merely becomes a shoulder on the copper peak. This situation is not acceptable for the determination of arsenic in high purity gold as there is a good chance of there being at least double the amount of copper than arsenic present. Ways of preventing copper interference would have to be considered.

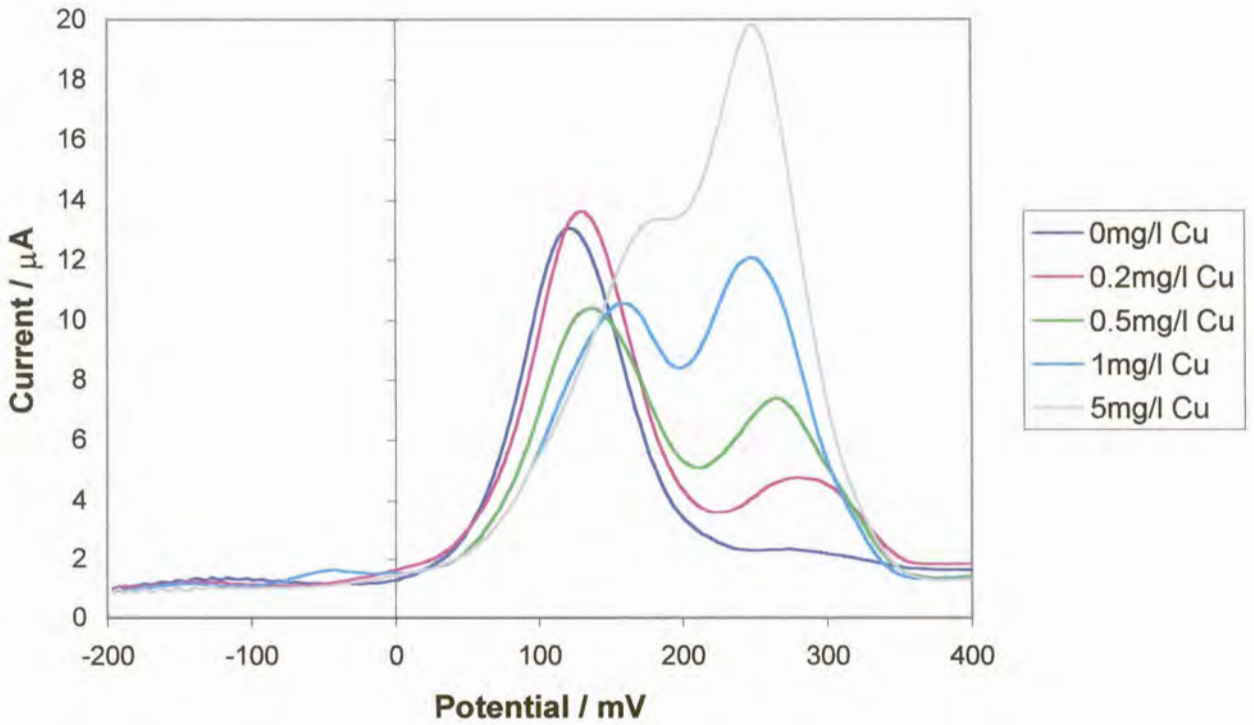

Figure 7.20: Voltammograms showing the effect of copper on the arsenic (III) peak

Interestingly, the copper peak does not seem to be affected by the arsenic present as the graph in figure 7.21 reveals. A linear graph is formed for concentrations up to 1 $mg.l^{-1}$ with a correlation coefficient of 0.9895.

It was not surprising that copper interfered with the arsenic determination. Apart from the oxidation peaks existing close together and overlapping, copper and arsenic combine strongly even in the presence of even a slight excess of copper and greatly reduces the arsenic response [13,29]. The fact that copper and arsenic form intermetallic compounds has been used to determine arsenic at a mercury electrode in the presence of copper [18].

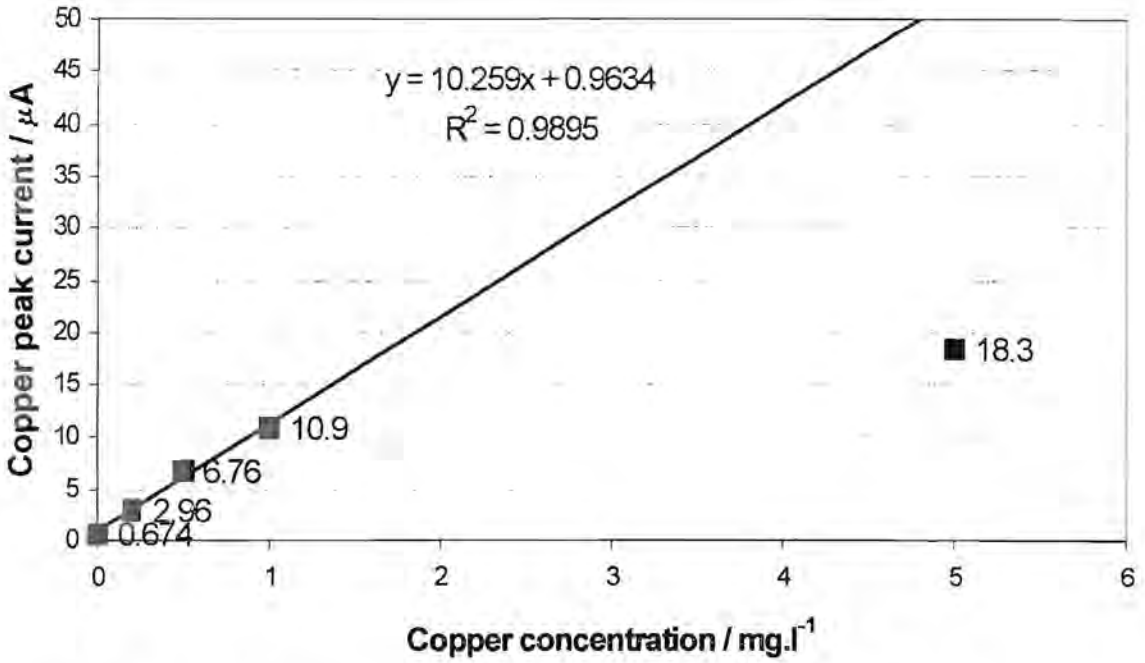

Figure 7.21: Graph of copper peak current versus copper concentration

7.5) DISCUSSION

The high purity gold could be dissolved in an alkaline cyanide solution in the presence of oxygen to form the gold (I) cyanide complex. This was to prevent the gold from depositing on the electrode simultaneously with the arsenic. Also, since cyanide is a reducing agent, arsenic would be present as arsenic (III) and thus a reduction step could be avoided.

It was found that using an alkaline solution produced interference from gold (I) cyanide and also lead to the passivation of the gold film electrode. Thus the sample solutions were adjusted to a pH of 3. Decomposition of the gold (I) cyanide complex was avoided by not using lower pH values. The optimum deposition potential was also found to be –650 mV, which produced sufficient reproducibility.

Matrix exchange was investigated in order to provide more sensitive arsenic determinations. Hydrochloric acid as a stripping electrolyte, of which a 4 $mol.l^{-1}$ solution was suggested, produced sensitive and reproducible results, but the linear range was fairly small. Sulphuric acid alone as a stripping

electrolyte yielded very poor sensitivity, but the addition of a small amount of hydrochloric acid appreciably improved the sensitivity. A larger linear range was obtained with the acid mixture when compared to that using hydrochloric acid alone. A composition of 2 $mol.l^{-1}$ sulphuric acid and 0.2 $mol.l^{-1}$ hydrochloric acid was recommended. Deciding which stripping electrolyte is best for the analysis would depend on the concentration of arsenic in the solution. If the arsenic concentration is low, hydrochloric acid would be the best to use due to the greater sensitivity. At higher arsenic concentrations, the sulphuric-hydrochloric acid mixture would be more suitable because of the greater linear range. A method of standard addition was required to reduce the memory effect displayed by the gold electrode and the samples had to be analysed in the order of increasing concentration.

Arsenic concentrations down to 0.1 $mg.l^{-1}$ could readily be detected using a 20 s deposition time for the hydrochloric acid stripping electrolyte or 60 s for the sulphuric-hydrochloric acid mixture. Lower concentrations were looked at, but insufficient sensitivity was obtained and increasing deposition times led to high background currents. In looking at the detection limit of the method, consider that 0.2 g gold was dissolved and the volume was made up to 20 ml. Assuming arsenic is present at 0.2 $mg.g^{-1}$ [37] in the gold sample, then 2.0 $\mu g.l^{-1}$ arsenic needs to be detected. Alternatively, an arsenic concentration of 10 $\mu g.g^{-1}$ in the gold sample can be detected if 0.2 g sample is dissolved in 20 ml of solution. The detection limit was not as low as that achieved by ICP-MS, which was 5 $\mu g.g^{-1}$ for arsenic [38], but was still sufficient to provide a valuable information for the typical arsenic concentrations in high purity gold up to 99.99% gold.

Cobalt, silver and copper were looked at as likely interferences. Cobalt and silver did not interfere when present at the concentration ratios likely to be found in high purity gold. Copper, however, interfered strongly due to the formation of intermetallic copper and arsenic [13,29]. The best way to curb this problem would be to complex the copper with a ligand that is stable and selective for copper, such as DMG. This would prevent intermetallic formation

and hence reduce interference. Cyanide forms a complex with copper, $[Cu(CN)4]^{2-}$, but it is not very stable (log β_4 = 31.3) [39] and it did not appear to affect the copper and arsenic interactions. As copper is present in high purity gold at concentrations which would lead to interference, the analysis of real samples was prevented as this interference would first have to be overcome.

7.6) REFERENCES

1) M.C. Sneed, J.L. Maynard and R.C. Brasted, Comprehensive Inorganic Chemistry, Volume II, D. von Nostrand company, USA, 1954
2) E. Guindy, Precious Metals, 6th International Conference, Pergamon Press, Toronto, Canada, 1983
3) D.W. Kirk, F.R. Foulkes and W.F. Graydon, J. Electrochem. Soc., 125 (1978) 1436
4) C.P. Thurgood, D.W. Kirk, F.R. Foulkes and W.F. Graydon, J. Electrochem. Soc., 128 (1981) 1680
5) D.W. Kirk, F.R. Foulkes and W.F. Graydon, J. Electrochem. Soc., 126 (1979) 2287
6) D.M. MacArthur, J. Electrochem. Soc., 119 (1972) 672
7) D.W. Kirk and F.R. Foulkes, J. Electrochem. Soc., 127 (1980) 1993
8) K.J. Cathro and D.F.A. Koch, J. Electrochem. Soc., 111 (1964) 1416
9) G.N. Gansinger, United States Patent No. 3989800, 1976
10) J.W. Mellor, A Comprehensive Treatise of Inorganic and Theoretical Chemistry, Volume II, Longmans, Green and Co., 1941
11) Gold Metallurgy in South Africa, Chamber of Mines of SA, Johannesburg, 1972
12) Y.-C. Sun, J. Mierzwa and M.-H. Yang, Talanta, 44 (1997) 1379
13) G. Forsberg, J.W. O'Laughlin, R.G. Megargle and S.R. Koirtyohann, Anal. Chem., 47 (1975) 1586
14) F.G. Bodewig, P. Valenta and H.W. Nurnberg, Fresenius Z. Anal. Chem., 311 (1982) 187
15) F.T. Henry and T.M. Thorpe, Anal. Chem., 52 (1980) 80

16) T.W. Hamilton, J. Ellis and T.M. Florence, Anal. Chim. Acta, 119 (1980) 225
17) F.T. Henry, T.O. Kirch and T.M. Thorpe, Anal. Chem., 51 (1979) 215
18) M. Kopanica and L. Novotny, Anal. Chim. Acta, 368 (1998) 211
19) I. Eguiarte, R.M. Alonso and R.M. Jimenez, Analyst, 121 (1996) 1835
20) D. Sancho, M. Vega, I. Deban, R. Pardo and G. Gonzalez, Analyst, 123 (1998) 743
21) P.H. Davis, G.R. Dulude, R.M. Griffin, W.R. Matson and E.W. Zink, Anal. Chem., 50 (1978) 137
22) S. Nielsen and E.H. Hansen, Anal. Chim. Acta, 343 (1997) 5
23) A.R.K. Dapaah and A. Ayame, Anal. Chim. Acta, 360 (1998) 43
24) S.B. Adeloju, T.M. Young, D. Jagner and G.E. Batley, Anal. Chim. Acta, 381 (1999) 207
25) P. Grundler and G.-U. Flechsig, Electrochim. Acta, 43 (1998) 3451
26) G. Henze, W. Wagner and S. Sander, Fresenius J. Anal. Chem, 358 (1997) 741
27) J.H. Aldstadt and A.F. Martin, Analyst, 121 (1996) 1387
28) A.J. Bard, Encyclopaedia of Electrochemistry of the Elements, Volume II, Marcel Dekker Inc., 1974
29) D. Jagner, M. Josefson and S. Westerlund, Anal. Chem., 53 (1981) 2144
30) J. Wang and B. Greene, J. Electroanal. Chem., 154 (1983) 261
31) T.M. Florence and G.E. Batley, Crit. Rev. in Anal. Chem., 9 (1980) 219
32) M. Lintern, A. Mann and D. Longman, Anal. Chim. Acta, 209 (1988) 193
33) F.R. Schlodder, H.H. Beyer and W.G. Zilske, Gold 100 Vol. 3, Proceedings of the Symposium on the Industrial uses of Gold, Johannesburg, SAIMM, 1986
34) P. Wilkinson, Gold Bulletin, 19 (1986) 75
35) G. Brauer, Handbook of Preparative Inorganic Chemistry, Volume 2, 2nd Edition, Academic Press, 1965
36) P.T. Kissinger and W.R. Heineman, Laboratory Techniques in Electroanalytical Chemistry, 2nd Edition, Marcel Dekker Inc, New York, 1996
37) E. Ivanova, N. Jordanov, I. Havesoz, M. Stoimenove and S. Kadieva, Fresenius J. Anal. Chem., 336 (1990) 501

38) S.M. Graham and R.V.D. Robert, Talanta, 41 (1994) 1369

39) B. Jamoussi, M. Zajzouf and B. Ben Hassine, Fresenius J. Anal. Chem., 356 (1996) 331

CHAPTER 8

CONCLUSION

The initial question of whether electroanalytical techniques would be suitable to determine trace impurities in complex matrices will be addressed at the end of this chapter once the work done in the project is first be examined. A conclusion will then be drawn from these findings.

Matrix exchange was used in both cases due to the complex nature of the samples. This improved the selectivity and the sensitivity of the determination by reducing interference and optimising the conditions for stripping. This involved designing flow cells and building up flow systems. The flow systems also produced improved mass transfer, they were fairly easy to use, the analysis time was faster (particularly with on-line deoxygenation) and the system was automated to an extent. FlowTEK provided easy control of the peristaltic pump and the selection valve used and it would have been ideal if it could also control the BAS software somewhat.

Two different flow systems were employed, each with their own pros and cons. Each system, however, had it own requirements and thus it was impossible to incorporate only all the positive aspects into one flow system. A balance was thus sought after.

Both segmented and non-segmented flow were employed. The non-segmented system could be controlled more rigorously whereas the compressibility in the segmented system created problems even when a back pressure was applied.

Oxygen was removed from solutions to prevent interference. This was achieved by passing the solutions through the semi-permeable silicone tubing surrounded by nitrogen. Diffusion of the oxygen through the tubing into the nitrogen atmosphere occurred due to a concentration gradient. This proved to be highly efficient and could

readily be used in flow systems. The extent of oxygen removal depended on the flow rate and at higher flow rates it was supplemented by sparging the solutions with nitrogen first, but this depends on the specific requirements. It did, however, complicate matters due to the time delay between introducing the sample into the system and the sample reaching the flow cell. The use of square wave voltammetry has been shown to reduce oxygen interference without the need for deoxygenating the solutions. This would be worthwhile investigating to reduce the complexity of the flow system.

Two different electrodes were utilised, namely a SMDE and a gold film electrode. The SMDE was easy to use, reproducible and there were no problems with surface effects. A flow cell was designed with mercury flow perpendicular to that of the solution for enhanced sensitivity, but the mercury drop was unstable at high flow rates or in a pulsating flow. For the gold film electrode it was difficult to plate a uniform gold film of good quality. It was found that plating the film in the diffusion-activated potential region produced the best results. It was not easy to activate the glassy carbon substrate uniformly and the reproducibility of the electrode was poor. The use of polishing and electrochemical regeneration produced different surface effects and led to variations in the voltammograms obtained. The gold film also suffered from memory effects and passivation, and had to be replated regularly. It could however be used in a wall-jet cell where the hydrodynamics is well-defined. Overall, the SMDE was preferred due to the reproducibility and the ease of use when compared to the gold film electrode, and probably most other film or solid electrodes for the analysis of complex samples. It cannot, however, be used in all instances and legislation prohibiting the use of mercury necessitates the use of other electrodes.

The use of electrochemical techniques has obviated the need for preliminary separations in the samples investigated. In this project both ASV and AdSV, with optimised deposition potentials and accumulation times, provided sufficient selectivity and sensitivity when used in conjunction with matrix exchange. The compositions of both the supporting and the stripping electrolytes are vital to improve the sensitivity and selectivity of the determination. This includes the nature of the components, their

concentrations an the pH of the solutions. The use of complexing agents when analysing complex matrices by electrochemical means is invaluable. In this work the major components in the samples, namely zinc and gold, were complexed to prevent interference. Cobalt as an analyte was complexed with DMG to make its determination at a mercury electrode possible and also improved the sensitivity. The interference by copper in the determination of arsenic could also possibly be removed by complexing it with DMG for example, so that its reduction potential is shifted. Cyclic voltammetry was an important tool for obtaining an overview of the electrochemical system and the interaction of the various components under different conditions.

In this project, cobalt was successfully determined in a synthetic zinc electrolyte with a detection limit of 0.2 $mg.l^{-1}$ using a 20 s accumulation time. Arsenic in the presence of high gold concentrations was determined down to 20 $\mu g.g^{-1}$ for a 20 s deposition time using a hydrochloric acid stripping electrolyte, or a 60 s deposition time using a sulphuric-hydrochloric acid mixture stripping electrolyte.

Thus it has been demonstrated that it is possible to apply electrochemical techniques for trace determination in complex matrices. However, the methods are very complex and matrix specific. Both the major and the minor components in the matrix could have profound influences on the analyte determination as demonstrated. It is not always easy to obtain detection limits in the low $\mu g.l^{-1}$ range. Due to the major method development that is required for this type of analysis and the extreme matrix dependence, it is not recommended for use in a non-routine laboratory. However it is well suited to monitor on-going processes and in a routine environment.